

**RESEARCH ARTICLE**

# Concatenated $\gamma$ -aminobutyric acid type A receptors revisited: Finding order in chaos

Vivian Wan Yu Liao<sup>1</sup>, Han Chow Chua<sup>1</sup>, Natalia Magdalena Kowal<sup>1,2</sup>, Mary Chebib<sup>1</sup>, Thomas Balle<sup>1</sup>, and Philip Kiaer Ahring<sup>1</sup>

**$\gamma$ -aminobutyric acid type A receptors (GABA<sub>A</sub>Rs), the major inhibitory neurotransmitter receptors in the mammalian central nervous system, are arguably the most challenging member of the pentameric Cys-loop receptors to study due to their heteromeric structure. When two or more subunits are expressed together in heterologous systems, receptors of variable subunit type, ratio, and orientation can form, precluding accurate interpretation of data from functional studies. Subunit concatenation is a technique that involves the linking of individual subunits and in theory allows the precise control of the uniformity of expressed receptors. In reality, the resulting concatemers from widely used constructs are flexible in their orientation and may therefore assemble with themselves or free GABA<sub>A</sub>R subunits in unexpected ways. In this study, we examine functional responses of receptors from existing concatenated constructs and describe refinements necessary to allow expression of uniform receptor populations. We find that dimers from two commonly used concatenated constructs,  $\beta$ -23- $\alpha$  and  $\alpha$ -10- $\beta$ , assemble readily in both the clockwise and the counterclockwise orientations when coexpressed with free subunits. Furthermore, we show that concatemers formed from new tetrameric  $\alpha$ -10- $\beta$ - $\alpha$ - $\beta$  and  $\alpha$ -10- $\beta$ - $\alpha$ - $\gamma$  constructs also assemble in both orientations with free subunits to give canonical  $\alpha\beta\gamma$  receptors. To restrict linker flexibility, we systematically shorten linker lengths of dimeric and pentameric constructs and find optimized constructs that direct the assembly of GABA<sub>A</sub>Rs only in one orientation, thus eliminating the ambiguity associated with previously described concatemers. Based on our data, we revisit some noncanonical GABA<sub>A</sub>R configurations proposed in recent years and explain how the use of some concatenated constructs may have led to wrong conclusions. Our results help clarify current contradictions in the literature regarding GABA<sub>A</sub>R subunit stoichiometry and arrangement. The lessons learned from this study may guide future efforts in understanding other related heteromeric receptors.**

## Introduction

$\gamma$ -aminobutyric acid type A receptors (GABA<sub>A</sub>Rs) belong to the Cys-loop superfamily of ligand-gated ion channels and are, as the name implies, gated by  $\gamma$ -aminobutyric acid (GABA; for a recent review, see Chua and Chebib [2017]). These receptors play significant physiological roles in the mammalian brain and are targets of a wide range of therapeutic drugs such as benzodiazepines and general anesthetics. Like other Cys-loop receptors, GABA<sub>A</sub>Rs are made up of five subunits encircling a central ion pore. While identical subunits can assemble to form homomeric receptors, it is more common for different subunits to form heteromeric receptor combinations (or subtypes). Evidence thus far suggests that binary, ternary, and quaternary receptors (i.e., receptors made up of two, three, or four different types of subunits, respectively) exist physiologically. Given the 19 mammalian GABA<sub>A</sub>R subunits ( $\alpha$ 1-6,  $\beta$ 1-3,  $\gamma$ 1-3,  $\delta$ ,  $\pi$ ,  $\epsilon$ ,  $\theta$ , and  $\rho$ 1-3) cloned to date, this gives rise to a multitude of possible

receptor subtypes. While the actual number of receptor subtypes expressed in vivo is less daunting than the theoretical maximum (Olsen and Sieghart, 2008), there is still a striking level of structural complexity that renders GABA<sub>A</sub>Rs one of the most challenging members of Cys-loop receptors to study.

As most ligand binding sites are found in interfaces between two subunits, pinning down the precise ratios of subunits and how they orient themselves spatially in each receptor subtype is a prerequisite for the accurate delineation of GABA<sub>A</sub>R function and pharmacology. Therefore, researchers have resorted to subunit concatenation to define subunit stoichiometry and arrangement of heterologously expressed GABA<sub>A</sub>Rs. This technique fuses subunit complementary DNAs (cDNAs) with a linker bridging the C terminus of the first subunit to the N terminus of the second subunit, thus allowing multiple subunits to be expressed together as one entity. Following the creation of the first

<sup>1</sup>The University of Sydney, Brain and Mind Centre, School of Pharmacy, Faculty of Medicine and Health, Camperdown, New South Wales, Australia; <sup>2</sup>Faculty of Pharmaceutical Sciences, School of Health Sciences, University of Iceland, Reykjavik, Iceland.

Correspondence to Philip Kiaer Ahring: [philip.ahring@sydney.edu.au](mailto:philip.ahring@sydney.edu.au).

© 2019 Liao et al. This article is distributed under the terms of an Attribution–Noncommercial–Share Alike–No Mirror Sites license for the first six months after the publication date (see <http://www.rupress.org/terms/>). After six months it is available under a Creative Commons License (Attribution–Noncommercial–Share Alike 4.0 International license, as described at <https://creativecommons.org/licenses/by-nc-sa/4.0/>).

concatenated  $\alpha 6$ - $\beta 2$  construct by Im et al. (1995), systematic refinements performed by the Sigel group in the early 2000s (Baumann et al., 2001, 2002; Minier and Sigel, 2004) have since popularized the use of concatenated constructs in the GABA<sub>A</sub>R field. Furthermore, the specific strategies devised by the Sigel group have strongly influenced how subunits are concatenated for nearly two decades (Baumann et al., 2003; Bracamontes and Steinbach, 2009; Kaur et al., 2009; Shu et al., 2012; Botzolakis et al., 2016).

Concatemers have contributed immensely to the understanding of assembly, function, and pharmacology of specific GABA<sub>A</sub>R subtypes. In the case of the  $\alpha 1\beta 2\gamma 2$  receptor, the most ubiquitous GABA<sub>A</sub>R in the human brain, data collected with the use of various dimeric, trimeric, tetrameric, and pentameric concatemers overwhelmingly support a  $(\alpha 1)_2(\beta 2)_2(\gamma 2)$  stoichiometry, with a subunit order of  $\beta\alpha\beta\alpha\gamma$  in a counterclockwise orientation when viewed extracellularly. Recent cryogenic electron microscopy structures have confirmed this stoichiometry (Zhu et al., 2018). The two  $\beta 2$ - $\alpha 1$  interfaces harbor GABA binding sites and the  $\alpha 1$ - $\gamma 2$  interface binds benzodiazepines and zolpidem. Hence, there appear to be rules governing the formation of GABA<sub>A</sub>Rs where certain subunits have specific roles and assembly preferences. However, conflicting results suggesting alternative assembly options have been reported recently. In a study conducted by Botzolakis et al. (2016),  $\alpha 1$  and  $\gamma 2$  subunits appeared to have the ability to substitute for a  $\beta 2$  subunit to give  $(\alpha 1)_3(\beta 2)(\gamma 2)$  ( $\beta\alpha\gamma\alpha\alpha$ ) and  $(\alpha 1)_2(\beta 2)(\gamma 2)_2$  ( $\beta\alpha\gamma\alpha\gamma$ ) receptors. Other studies have reported that  $\gamma$  and  $\delta$  subunits might substitute for an  $\alpha$  subunit leading to functional binary  $\beta\gamma$  and  $\beta\delta$  receptors (Chua et al., 2015; Lee et al., 2016; Wongsamitkul et al., 2017). Hence, these studies raise the possibility of substantial heterogeneity in the formation of GABA<sub>A</sub>Rs.

While the concatenation technique is powerful, there are also caveats associated with its use. In a review by Ericksen and Boileau (2007), a number of these caveats were discussed for the Cys-loop receptor field including proteolysis, optimal linker length, clockwise versus counterclockwise concatemer assembly and loop-outs. Perplexingly, some of the key points of this review appear to have been largely ignored in the field, perhaps because they were only backed by in silico modeling. Sigel et al. (2009) later discussed the potential pitfalls specifically relating to the GABA<sub>A</sub>R constructs designed by his group. This included nonoptimal linker design and whether signal-peptide sequences in downstream linked subunits should be omitted; however, the possibility for clockwise as well as counterclockwise concatemer assembly was not mentioned. Recently, we discovered that expression of published concatenated nicotinic acetylcholine receptor (nAChR) constructs in *Xenopus laevis* oocytes led to far more complex receptor pools than anticipated (Ahring et al., 2018). This was due to an ability of the linked concatemers to orient themselves in both the clockwise and the counterclockwise directions. Due to this flexibility, receptor pools contained mixtures of receptors with different stoichiometries whenever ternary scenarios were examined. Most importantly, we additionally determined that optimized linker lengths can lead to uniform nAChR receptor pools where functional receptors

primarily originate from concatemers assembled in the counterclockwise orientation.

In this present study, we shift the focus to concatenated GABA<sub>A</sub>Rs to evaluate whether previously designed GABA<sub>A</sub>R constructs give uniform resultant receptor pools. As expected, based on our previous work on the nAChRs, this is not the case. Dimeric constructs and tetrameric constructs thereof lead to dimers and tetramers, which have the inherent ability to assemble in both the clockwise and the counterclockwise orientations. In an attempt to constrain this flexibility, we design a range of dimeric and pentameric constructs with systematically shortened linker lengths. We show that it is possible to obtain a uniform receptor pool of ternary GABA<sub>A</sub>Rs using new optimized concatenated constructs. Our work implies that previous conclusions based on data from concatenated constructs may need to be reexamined. Based on our findings, we conclude that GABA<sub>A</sub>R assembly may be less chaotic than proposed in recent studies.

## Materials and methods

Zolpidem was purchased from Toronto Research Chemicals. GABA, kanamycin, theophylline, collagenase, HEPES, and all salts or other chemicals not specifically mentioned were purchased from Sigma-Aldrich and were of analytical grade. Oligonucleotides were purchased from Sigma-Aldrich, and sequencing services were from Australian Genome Research Facility. Restriction enzymes, Q5 polymerase, T4 DNA ligase, and 10-beta competent *Escherichia coli* were from New England Biolabs. DNA purification kits were from Qiagen. The QuickChange II Site-Directed Mutagenesis kit was from Agilent Technologies, and the mMessage mMachine T7 transcription kit was from ThermoFisher Scientific.

## Molecular biology

Human cDNA for wild-type monomeric  $\alpha 1$ ,  $\beta 2$ , and  $\gamma 2$ s GABA<sub>A</sub>R subunits and a concatenated construct thereof,  $\beta 2$ -23- $\alpha 1$ , were kind gifts from Saniona A/S. Naturally occurring BamHI, HindIII, and KpnI restriction sites in the  $\alpha 1$  and  $\beta 2$  subunit sequences, which would interfere with the concatenation strategy, were initially removed by silent mutations using site-directed mutagenesis. In the following, amino acids are represented by their single-letter code. Point mutated  $\gamma 2^{A79R}$  and  $\alpha 1^{R67A}$  subunits were likewise prepared using site-directed mutagenesis. The numbering convention used is based on the mature peptide sequences (i.e., after signal peptide cleavage). A79 corresponds to the A118 residue in the full-length  $\gamma 2$  cDNA sequence, and R67 corresponds to the R94 residue in the full-length  $\alpha 1$  cDNA sequence based on sequence information from UniProt with accession nos. P18507 and P14867, respectively. Note that the two  $\gamma 2^{A79R}$  and  $\alpha 1^{R67A}$  mutants essentially swap the homologous loop D residues between these two subunits.

To generate new concatenated  $\alpha 1$ -xa- $\beta 2$  constructs, where x represents the number of amino acids (a) added or deleted while linking the subunits, specific linker sequences and cloning restriction sites were added to the  $\alpha 1$  and  $\beta 2$  cDNAs before the final assembly procedure. In brief, AGS linker sequences were

designed to contain a unique BamHI restriction site (embedded in codons for GS) and antisense  $\alpha 1$  as well as sense  $\beta 2$  oligonucleotide sequences were fabricated to traverse this site. The antisense  $\alpha 1$  oligonucleotides caused in-frame fusion of the last amino acid in  $\alpha 1$  (PTPHQ<sup>456</sup>) to the AGS linker sequence. The sense  $\beta 2$  oligonucleotides caused in-frame fusion of the AGS linker sequence to the first amino acid in the predicted mature  $\beta 2$  (Q<sup>25</sup>SVND) peptide (omission of the  $\beta 2$  signal peptide). The remaining oligonucleotides were designed to match the respective wild-type sequences and include suitable restriction sites for cloning purposes. Standard PCR reactions with  $\alpha 1$  or  $\beta 2$  as template were performed using Q5 polymerase, and PCR products were cloned into in-house vectors using restriction digestion and ligation. Correct introduction of linker sequences and fidelity of all coding sequences were then verified by double-stranded sequencing. Thereafter, concatenated constructs were created by restriction digestion and ligation using the unique AGS linker BamHI site. The  $\alpha 1$ -10- $\beta 2$  ( $\alpha 1$ -LQ<sub>9</sub>- $\beta 2$ ) construct was built in a similar manner with the linker sequence containing a unique PstI restriction site (embedded in codons for LQ). Likewise, tetrameric and pentameric constructs of  $\alpha 1$ ,  $\beta 2$ , and  $\gamma 2$ s subunits were built by using 3–4 different linker sequences where each contained either a unique BamHI (embedded in codons for GS), HindIII (embedded in codons for GSL), KpnI (embedded in codons for GT), or AgeI (embedded in codons for TG) restriction site (Table 3). *E. coli* 10-beta bacteria were used as hosts for plasmid amplification, and plasmid purifications were performed with standard kits (Qiagen). Complementary RNA (cRNA) was produced from linearized cDNA using the mMessage mMachine T7 Transcription kit according to the manufacturer's descriptions and stored at  $-80^{\circ}\text{C}$  until use. For tetrameric and pentameric constructs, which represent long transcripts, the guanosine triphosphate concentration was increased to give a final cap analog ( $\text{m}^7\text{G}(5')\text{ppp}(5')\text{G}$ ) to guanosine triphosphate ratio of 2:1.

### Modeling

A homology model of an  $\alpha 1$ - $\beta 2$ - $\alpha 1$  trimer was constructed using a human GABA<sub>A</sub>R  $\beta 3$  homo-pentamer as template (Miller and Aricescu, 2014). The template x-ray structure (PDB accession no. 4COF) was downloaded from the RCSB Protein Data Bank ([www.rcsb.org](http://www.rcsb.org)) and prepared following the protocol for protein preparation implemented in Maestro 11.2 (Schrödinger Release 2017–2: Maestro, Schrödinger). Query sequences for the human  $\alpha 1$  and  $\beta 2$  GABA<sub>A</sub>Rs were obtained from UniProt with accession nos. P14867 and P47870, respectively. Signal peptides, the second intracellular loop, and C-terminal tails, for which no template exists in the 4COF structure, were deleted from the sequences. Query sequences were then aligned to chains E, A, and B of the template to give the  $\alpha 1$ - $\beta 2$ - $\alpha 1$  trimer. Twenty models were constructed using Prime, and the model with the best Prime score was selected for further refinement involving loop sampling of the  $\beta 2$  N terminus. To illustrate linker orientations, the disordered N-terminal part of the  $\beta 2$  subunit was sculpted toward the C terminus of the neighboring  $\alpha 1$  subunits in the clockwise and counterclockwise directions, respectively. The gap between the last modeled residue in the  $\alpha 1$  C terminus

(WATYL<sup>443</sup>) and the  $\beta 2$  N terminus was subsequently bridged with AGS repeats in such a way that a subsequent geometry optimization (Macromodel) did not lead to significant distortion or displacement of helices at either end of the linker.

### Expression of GABA<sub>A</sub>Rs in *X. laevis* oocytes

Oocytes were obtained and prepared as previously described (Mirza et al., 2008). Briefly, to obtain isolated oocytes, lobes from ovaries were removed from anesthetized adult female *X. laevis* frogs following a protocol approved by the Animal Ethics Committee of The University of Sydney (reference number: 2013/5915). To obtain isolated oocytes, ovary lobes were sliced into small pieces using surgical knives and defolliculated by collagenase treatment. Stage V and VI oocytes were injected with  $\sim 50$  nl of a 0.5 ng/nl cRNA mixture encoding the desired GABA<sub>A</sub>R subunits and incubated for 3–5 d at  $18^{\circ}\text{C}$  in modified Barth's solution (96 mM NaCl, 2.0 mM KCl, 1 mM MgCl<sub>2</sub>, 1.8 mM CaCl<sub>2</sub>, 5 mM HEPES, 2.5 mM sodium pyruvate, 0.5 mM theophylline, and 100  $\mu\text{g}/\text{ml}$  gentamycin; pH 7.4).

### Electrophysiology

Electrophysiological recordings using the two-electrode voltage-clamp technique were performed as described previously (Mirza et al., 2008; Ahring et al., 2016; Kowal et al., 2018). Briefly, oocytes were placed in a custom-built recording chamber and continuously perfused with a saline solution termed ND96 (96 mM NaCl, 2 mM KCl, 1 mM MgCl<sub>2</sub>, 1.8 mM CaCl<sub>2</sub>, and 10 mM HEPES; pH 7.4). Pipettes were backfilled with 3 M KCl, and open pipette resistances ranged from 0.4 to 2 M $\Omega$  when submerged in ND96 solution. Cells were voltage clamped at a holding potential of  $-60$  mV using an Axon GeneClamp 500B amplifier (Molecular Devices). Oocytes with initial leak currents exceeding 300 nA when clamped were discarded. Amplified currents were filtered at 20 Hz by a four-pole low-pass Bessel filter (Axon GeneClamp 500B), digitized by a Digidata 1440A (Molecular Devices), and sampled at 200 Hz as well as analyzed on a personal computer using the pClamp 10.2 suite (Molecular Devices). Responses to individual applications were collected as episodic traces following triggering events.

GABA was dissolved in ultrapure water at a concentration of 316 mM, while zolpidem was dissolved as a 100-mM stock solution in DMSO. The maximal concentration of DMSO in perfusates was always  $<0.1\%$  and this did not evoke any measurable currents from wild-type  $\alpha 1\beta 2\gamma 2$  receptors. Stock solutions were stored at  $-20^{\circ}\text{C}$ . Fresh GABA and zolpidem dilutions were prepared in ND96 solution on the day of the experiment. To ensure rapid solution exchange in the immediate oocyte vicinity, a 1.5-mm diameter capillary tube was placed  $\sim 2$  mm from the oocyte. By way of this capillary tube, oocytes were continuously perfused with saline ND96 solution or test application at a flow rate of 2.0 ml/min. Each application lasted  $\sim 30$  s and was followed by a 2–5-min washout period depending on the ligand concentration of a given application.

### Experimental protocols

To determine the concentration–response relationships (CRRs) of different constructs, five to seven concentrations of GABA or

zolpidem were applied to each oocyte. To ensure reproducibility of evoked current amplitudes, a set of control applications was performed before the CRR experiments. These were as follows: three GABA<sub>control</sub> (2–100 μM; approximately EC<sub>5-30</sub> depending on receptor type) applications, one GABA<sub>max</sub> (316–10,000 μM; approximately EC<sub>100</sub>) application, and another three GABA<sub>control</sub> applications. Increasing concentrations of GABA alone or zolpidem coapplied with GABA<sub>control</sub> were applied after the control experiments. Final datasets for GABA and zolpidem were assembled from a minimum of five experiments conducted on a minimum of two batches of oocytes. Single data points were generally not excluded from calculations; instead, all data from oocytes with incomplete CRRs or erratic control GABA responses were excluded.

### Data analysis

Raw traces were analyzed using pClamp 10.2 (Molecular Devices). During analysis, episodic traces for each individual application were overlaid and baseline subtracted. Peak current amplitudes were quantified by measuring the maximum inward current for each response. For GABA CRR experiments, peak current amplitudes (*I*) of all responses were fitted to the Hill equation and then normalized to the maximal fitted response (*I*<sub>max\_fit\_GABA</sub>) for each individual oocyte (*I*/*I*<sub>max\_fit\_GABA</sub>). For experiments with zolpidem, the compound was coapplied with GABA<sub>control</sub> (2–100 μM). Differences between GABA<sub>control</sub>-evoked current amplitudes in the absence or presence of zolpidem (*I*) were calculated as the percentage change from the GABA<sub>control</sub>-evoked current: that is,  $([I - I_{GABA\_control}] \times 100) / I_{GABA\_control}$ . The calculated zolpidem responses for each oocyte were then fitted to the Hill equation and normalized to the maximal fitted response (*I*<sub>max\_fit\_zolpidem</sub>). All CRRs were fitted by nonlinear regression to the Hill equation using GraphPad Prism 7. Unless otherwise specified, a simple monophasic model with three variables was used (i.e., fixed Hill slope of 1), and efficacy at infinitely low compound concentrations was set to 0. The model with fixed Hill slope was chosen universally over a variable slope model for two main reasons: first, it represented the statistically better choice for the majority of the datasets according to the extra sum-of-squares F test; and second, it limits overinterpretation of data in cases where Hill slopes differ substantially from 1 due to mixed receptor pools. Statistical analysis was performed using GraphPad Prism 7.

## Results

In the present study, we performed analysis of receptors arising from previously published as well as new concatenated GABA<sub>A</sub>R constructs. *X. laevis* oocytes were injected with ~25 ng of the respective cRNA mixtures and incubated for 2–6 d before subjection to two-electrode voltage-clamp electrophysiology. The maximal GABA-evoked (GABA<sub>max</sub>) peak-current amplitude and a full GABA CRR were obtained at each individual oocyte. In cases where the cRNA mixture contained a γ2 subunit, the dataset was complemented with full CRRs for zolpidem. The aim of the zolpidem experiments is to assess for potential changes in modulatory potency and most data are therefore normalized.

Note that SD error is used in the graphical representation of CRRs, as the relatively minor variabilities often resulted in SEM error bars being hidden by the data symbols.

### GABA and zolpidem CRRs at wild-type α1β2 and α1β2γ2 receptors

Like many other Cys-loop receptors, binary α1β2 GABA<sub>A</sub>R<sub>s</sub> can express in two stoichiometries, (α1)<sub>2</sub>(β2)<sub>3</sub> or (α1)<sub>3</sub>(β2)<sub>2</sub> (Baumann et al., 2001; Boileau et al., 2005; Che Has et al., 2016). To obtain expression of receptor populations enriched in one or the other of these stoichiometries, α1 and β2 cRNAs were mixed in a biased 1:50 or 50:1 ratio. The α1β2γ2 receptor was expressed using a biased cRNA ratio of 5:1:5 to ensure enrichment of (α1)<sub>2</sub>(β2)<sub>2</sub>(γ2) receptors (Hartiadi et al., 2016).

The GABA CRRs at (α1)<sub>2</sub>(β2)<sub>3</sub> and (α1)<sub>3</sub>(β2)<sub>2</sub> receptors were virtually identical with resulting fitted half maximal effective concentration (EC<sub>50</sub>) values of 2.6 and 3.3 μM, respectively (Fig. 1 A and Table 1). Incorporation of a γ2 subunit into the receptor complex caused an ~10-fold decrease in the GABA potency resulting in a fitted EC<sub>50</sub> value of 22 μM for (α1)<sub>2</sub>(β2)<sub>2</sub>(γ2) receptors. Average GABA<sub>max</sub>-evoked peak-current amplitudes were in the range of 0.8–1.5 μA for the α1β2 receptor stoichiometries, whereas larger currents of ~3 μA were observed once the γ2 subunit was integrated (Fig. 1 B and Table 1). No effect of zolpidem was noted at either of the α1β2 receptor stoichiometries, whereas the compound was a potent positive modulator at the α1β2γ2 receptor with an EC<sub>50</sub> value of 0.11 μM (Fig. 1 C and Table 2). These data for GABA and zolpidem are generally in good agreement with literature reports (Boileau et al., 2005). In a recent report by Che Has et al. (2016), zolpidem modulation was observed at α1β3 receptors in the 3α:2β stoichiometry; however, these findings could not be reproduced with the conditions used here.

### Concatemers from the dimeric β-23-α and α-10-β constructs can assemble in both the clockwise and the counterclockwise orientations

To evaluate the expression and assembly pattern of concatenated GABA<sub>A</sub>R constructs, we initially tested two dimeric constructs termed β2-23-α1 and α1-10-β2 (β-23-α and α-10-β hereafter). These were originally designed by the Sigel group and have been widely used in the field (Baumann et al., 2001; Bracamontes and Steinbach, 2009; Shu et al., 2012; Botzolakis et al., 2016). The naming scheme indicates the number of amino acids used to connect the C terminus of the first subunit to the mature N terminus of the second subunit. The original linkers contained primarily glutamine (Q) repeats, and in our replica constructs either an identical [β-23-α, Q<sub>3</sub>(Q<sub>2</sub>A<sub>3</sub>PA)<sub>2</sub>AQ<sub>5</sub>] or virtually identical (α-10-β, LQ<sub>9</sub> instead of Q<sub>10</sub>) linker sequence was used (Table 3). Oocytes were injected with cRNA for the dimer constructs by themselves or in combinations with β2 or γ2 in a 1:1 ratio.

#### Dimeric constructs alone

Injection of cRNAs for β-23-α or α-10-β led to GABA<sub>max</sub>-evoked currents with average peak current amplitudes in the range of 0.5–0.8 μA (Fig. 2 A and Table 1). Hence, expressed dimers are



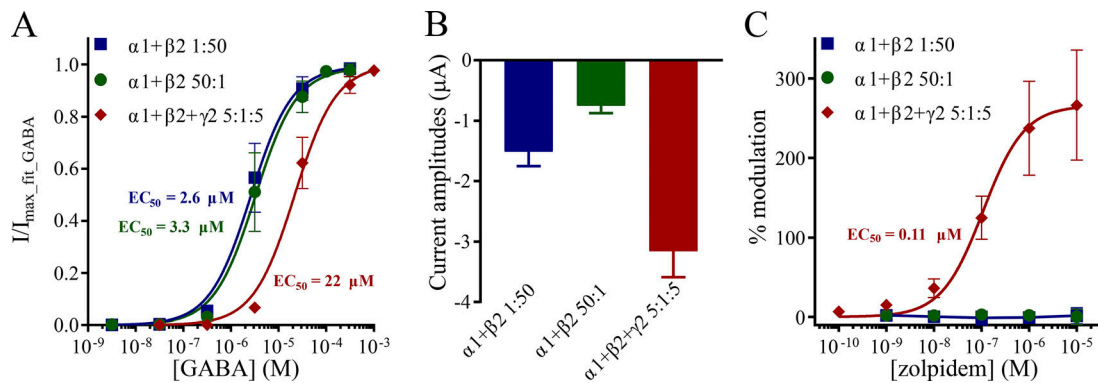


**Figure 1. Potency of GABA and zolpidem at  $\alpha 1\beta 2$  and  $\alpha 1\beta 2\gamma 2$  GABA<sub>A</sub>Rs.** *X. laevis* oocytes were injected with cRNA mixtures of  $\alpha 1$ ,  $\beta 2$ , and  $\gamma 2$  subunits in the indicated ratios and subjected to two-electrode voltage-clamp electrophysiology as described in the Materials and methods. Biased cRNA ratios were used to ensure enriched populations of  $(\alpha 1)_3(\beta 2)_2$ ,  $(\alpha 1)_2(\beta 2)_3$ , and  $(\alpha 1)_2(\beta 2)_2(\gamma 2)$  receptors. An approximate total of 25 ng cRNA was injected in a volume of 50 nl. **(A)** Baseline subtracted GABA-evoked peak-current amplitudes ( $I$ ) for receptors from the indicated cRNA mixtures were fitted to the Hill equation by nonlinear regression and normalized to the maximal fitted values ( $I_{\max\_fit\_GABA}$ ). Normalized responses are depicted as mean  $\pm$  SD as a function of the GABA concentration (in M), and they are fitted to the Hill equation with a fixed bottom of 0 and a Hill slope of 1. Data were obtained from  $n = 10$ –17 experiments, and regression results are presented in Table 1. **(B)** GABA<sub>max</sub>-evoked peak-current amplitudes from the experiments in A are depicted as means  $\pm$  SEM and calculated averages are presented in Table 1. A GABA concentration of 316  $\mu M$  was used as GABA<sub>max</sub>. **(C)** Zolpidem enhancement of GABA-evoked currents was evaluated for  $(\alpha 1)_3(\beta 2)_2$ ,  $(\alpha 1)_2(\beta 2)_3$ , and  $(\alpha 1)_2(\beta 2)_2(\gamma 2)$  receptors by co-application with a submaximal control concentration of GABA (2–5  $\mu M$ ). Baseline subtracted peak-current amplitudes ( $I$ ) were expressed as percent change from  $I_{GABA\_control}$  (% modulation) and are depicted as means  $\pm$  SD as a function of the zolpidem concentration (in M). Data points were fitted by nonlinear regression to the Hill equation with a fixed bottom of 0 and Hill slope of 1. The maximal fitted response for the  $\alpha 1\beta 2\gamma 2$  receptor was 270%  $\pm$  10%, whereas no positive modulation was observed at the two  $\alpha 1\beta 2$  receptors. Data were obtained from  $n = 6$ –11 experiments and regression results are presented in Table 2.

clearly able to assemble into functional pentameric receptors. GABA CRRs revealed fitted  $EC_{50}$  values of 3.0 and 2.8  $\mu M$  for  $\beta$ -23- $\alpha$  and  $\alpha$ -10- $\beta$ , respectively (Fig. 2, B and C; and Table 1). This is in good agreement with the 2.6–3.3- $\mu M$  range observed for  $(\alpha 1)_2(\beta 2)_3$  and  $(\alpha 1)_3(\beta 2)_2$  receptors obtained with biased cRNA ratios (Fig. 1 A) and suggests that these dimers form receptors that behave like regular  $\alpha 1\beta 2$  receptors formed from free subunits. Disregarding the possibility of linker proteolysis, the simplest explanation for these observations is that three dimers come together to form a pentameric receptor with one dangling subunit. As it is unknown whether the linkers direct the assembly orientation, there are six possible assemblies leading to receptors with two GABA-binding  $\beta 2$ - $\alpha 1$  interfaces for each construct (Fig. 3 A; note only  $\beta$ -23- $\alpha$  is depicted, but a similar scenario exists for  $\alpha$ -10- $\beta$ ). These have the linked subunits oriented in either the clockwise, the counterclockwise, or both orientations.

#### Dimeric constructs + $\beta 2$

Coinjection of  $\beta$ -23- $\alpha$  or  $\alpha$ -10- $\beta$  with free  $\beta 2$  subunits led to larger average GABA<sub>max</sub>-evoked peak current amplitudes in the 2- $\mu A$  range (Fig. 2 A and Table 1). This indicates that pentameric receptor assembly is more efficient when dimers are mixed with a free subunit, although the two- to fourfold difference appears relatively modest. The GABA CRRs are virtually identical for the two combinations, and the fitted  $EC_{50}$  values of 1.8–2.6  $\mu M$  are in good agreement with the value obtained for  $(\alpha 1)_2(\beta 2)_3$  using a biased cRNA ratio (Fig. 2, B and C; and Table 1). The simplest explanation for these observations is that two dimers form receptors with one  $\beta 2$  subunit. Given that the linkers may adopt the clockwise and/or counterclockwise orientations, there are

three assembly possibilities for each construct that all yield uniform 2 $\alpha$ :3 $\beta$  stoichiometry receptors.

#### Dimeric constructs + $\gamma 2$

Coinjection of  $\beta$ -23- $\alpha$  or  $\alpha$ -10- $\beta$  with  $\gamma 2$  led to substantially larger GABA<sub>max</sub>-evoked peak-current amplitudes in the  $\sim 8$ - $\mu A$  range (Fig. 2 D and Table 1). The fourfold amplitude increase compared with  $\beta 2$  coinjections could be due to a larger single-channel conductance observed for  $\gamma 2$ -containing receptors and/or increased translocation of receptors to the oocyte cell surface when a  $\gamma 2$  subunit is included (Angelotti and Macdonald, 1993; Mortensen and Smart, 2006). The GABA CRRs are similar for the two construct combinations with fitted  $EC_{50}$  values in the 9.2–14- $\mu M$  range (Fig. 2, E and F; and Table 1). These values are approximately twofold more potent than the 22  $\mu M$  obtained for  $(\alpha 1)_2(\beta 2)_2(\gamma 2)$  using a biased cRNA ratio, which might suggest that receptor pools contain a small percentage of pollutant binary  $\alpha 1\beta 2$  receptors. The modulatory potency of zolpidem is in the 0.1–0.18- $\mu M$  range, irrespective of whether receptors originate from free subunits or cRNA combinations with the concatenated constructs (Fig. 1 C; Fig. 2, G and H; and Table 2). While there are potentially three simple explanations for how each dimer could assemble with a  $\gamma 2$  subunit, only one led to canonical receptors that contain two GABA-binding  $\beta 2$ - $\alpha 1$  interfaces and one zolpidem-binding  $\alpha 1$ - $\gamma 2$  interface (Fig. 3 B, receptor 1 and 4). The other two assembly possibilities result in receptors with only one GABA-binding interface and it is questionable whether these are functional (addressed further below). Interestingly, to yield canonical receptors, the dimer linkers have to be orientated in a counterclockwise orientation for  $\beta$ -23- $\alpha$  +  $\gamma 2$  but a clockwise orientation for  $\alpha$ -10- $\beta$  +  $\gamma 2$ .

Table 1. Regression results from fitted GABA-evoked responses at wild-type and concatenated GABA<sub>A</sub>Rs

Construct	Subunit	GABA				n	GABA <sub>max</sub> (nA)
		E <sub>max</sub>	EC <sub>50</sub> (μM)	pEC <sub>50</sub>			
α1 + β2 1:50		0.99 ± 0.01	2.6	5.58 ± 0.03	12	1,500 ± 200	
α1 + β2 50:1		0.99 ± 0.02	3.2	5.49 ± 0.03	17	750 ± 120	
α1 + β2 + γ2 5:1:5		1.00 ± 0.01	22	4.66 ± 0.03	10	3,200 ± 400	
Dimeric constructs							
β2-23-α1		1.00 ± 0.02	3.0	5.53 ± 0.04	12	480 ± 100	
β2-23-α1	β2	1.00 ± 0.02	2.6	5.58 ± 0.03	10	1,900 ± 200	
β2-23-α1	γ2	1.00 ± 0.02	9.2	5.04 ± 0.04	8	8,400 ± 600	
α1-10-β2		1.00 ± 0.01	2.8	5.55 ± 0.03	11	820 ± 190	
α1-10-β2	β2	1.00 ± 0.01	1.8	5.75 ± 0.02	13	1,800 ± 200	
α1-10-β2	γ2	1.00 ± 0.02	14	4.84 ± 0.04	10	8,100 ± 600	
α1-9a-β2		1.00 ± 0.01	3.2	5.49 ± 0.03	10	190 ± 60	
α1-9a-β2	β2	1.00 ± 0.02	1.7	5.77 ± 0.04	11	1,200 ± 300	
α1-9a-β2	γ2	0.99 ± 0.01	17	4.77 ± 0.03	20	11,000 ± 1,000	
α1-6a-β2		0.99 ± 0.01	5.7	5.24 ± 0.03	11	140 ± 30	
α1-6a-β2	β2	1.00 ± 0.01	2.3	5.65 ± 0.02	11	1,300 ± 300	
α1-6a-β2	γ2	1.00 ± 0.02	41	4.38 ± 0.04	10	3,100 ± 300	
α1-3a-β2		1.00 ± 0.02	10	4.99 ± 0.04	10	89 ± 28	
α1-3a-β2	β2	1.00 ± 0.02	3.2	5.49 ± 0.03	9	630 ± 110	
α1-3a-β2	γ2	0.99 ± 0.02	34	4.46 ± 0.04	12	4,300 ± 500	
α1-0a-β2		N/A			19	34 ± 10	
α1-0a-β2	β2	1.00 ± 0.01	3.5	5.45 ± 0.02	14	630 ± 100	
α1-0a-β2	γ2	0.99 ± 0.03	130	3.88 ± 0.05	11	500 ± 140	
α1-(-1a)-β2		N/A			21	No current	
α1-(-1a)-β2	β2	0.99 ± 0.01	2.6	5.58 ± 0.03	7	400 ± 140	
α1-(-1a)-β2	γ2	0.99 ± 0.02 <sup>a</sup>	140 <sup>a</sup>	3.84 ± 0.04 <sup>a</sup>	18	7.8 ± 1.9 <sup>b</sup>	
α1-(-2a)-β2		N/A			15	No current	
α1-(-2a)-β2	β2	1.00 ± 0.01	2.6	5.59 ± 0.03	11	470 ± 90	
α1-(-2a)-β2	γ2	1.00 ± 0.01 <sup>a</sup>	130 <sup>a</sup>	3.90 ± 0.03 <sup>a</sup>	17	8.0 ± 3.6 <sup>b</sup>	
α1-(-3a)-β2		N/A			21	No current	
α1-(-3a)-β2	β2	0.96 ± 0.04	4.0	5.40 ± 0.08	8	40 ± 9	
α1-(-3a)-β2	γ2	1.00 ± 0.01 <sup>a</sup>	64 <sup>a</sup>	4.20 ± 0.02 <sup>a</sup>	24	2.3 ± 0.9 <sup>b</sup>	
Tetrameric constructs							
α1-10-β2-α1-β2		N/A			13	60 ± 13	
α1-10-β2-α1-β2	γ2	0.99 ± 0.02	32	4.50 ± 0.03	17	6,500 ± 1,000	
α1-10-β2-α1-γ2		N/A			15	150 ± 25	
α1-10-β2-α1-γ2	β2	0.96 ± 0.03	34	4.47 ± 0.05	19	4,700 ± 400	
Pentameric constructs							
α1-(-1a)-β2-α1-β2-γ2		0.99 ± 0.01	390	3.41 ± 0.02	19	320 ± 40	
α1-(-1a)-β2-α1-γ2-β2		1.00 ± 0.01	330	3.49 ± 0.02	16	3,500 ± 400	
γ2-15a-β2-α1-β2-α1		0.99 ± 0.03	51	4.30 ± 0.04	11	4,900 ± 600	
γ2-13a-β2-α1-β2-α1		0.99 ± 0.02	70	4.16 ± 0.03	12	5,300 ± 500	
γ2-11a-β2-α1-β2-α1		0.99 ± 0.01	110	3.96 ± 0.02	17	3,300 ± 500	
γ2-10a-β2-α1-β2-α1		0.99 ± 0.02	120	3.92 ± 0.04	10	3,100 ± 700	

Table 1. Regression results from fitted GABA-evoked responses at wild-type and concatenated GABA<sub>A</sub>Rs (Continued)

Construct	Subunit	GABA			n	GABA <sub>max</sub> (nA)
		E <sub>max</sub>	EC <sub>50</sub> (μM)	pEC <sub>50</sub>		
γ2-9a-β2-α1-β2-α1		1.00 ± 0.01	120	3.92 ± 0.02	15	890 ± 160
Mutant constructs						
α1-9a-β2	γ2(A118R)	0.99 ± 0.02	30	4.52 ± 0.04	13	8,700 ± 1,500
α1-0a-β2	γ2(A118R)	1.00 ± 0.01	110	3.98 ± 0.02	9	600 ± 90
α1 <sup>R94A</sup> + β2 + γ2 5:1:5		0.99 ± 0.02	1,100 <sup>c</sup>	2.97 ± 0.03 <sup>c</sup>	10	7,100 ± 400
γ2-11a-β2-α1-β2-α1 <sup>R94A</sup>		1.01 ± 0.01	2,600 <sup>c</sup>	2.58 ± 0.02 <sup>c</sup>	14	3,600 ± 300
γ2-11a-β2-α1-β2-α1 <sup>R94A</sup>	α1	0.97 ± 0.02 <sup>c,d</sup>	2,000 <sup>c,d</sup>	2.70 ± 0.03 <sup>c,d</sup>	12	1,700 ± 200

Data points were fitted to the Hill equation with the bottom set to 0 and Hill slope set to 1 by nonlinear regression. Normalized fitted maximal responses of GABA are presented as E<sub>max</sub> ± SEM. Fitted potencies of GABA are presented as EC<sub>50</sub> in μM and pEC<sub>50</sub> ± SEM where p = -Log for the indicated number (n) of individual oocytes. The average maximal current obtained with GABA<sub>max</sub> applications is presented as GABA<sub>max</sub> ± SEM in nA for the tested oocytes. For α-10-β+γ2, a GABA concentration of 3,160 μM was used to establish GABA<sub>max</sub>-evoked peak currents amplitudes, whereas a concentration of 316 μM was used for all remaining cRNA combinations of wild-type free subunits, binary constructs, and tetrameric constructs. For pentameric constructs and cRNA combinations with mutant subunits, the GABA<sub>max</sub> concentration was adjusted according to the EC<sub>50</sub> value of GABA CRRs: for CRRs with EC<sub>50</sub> values <70 μM, a concentration of 316 μM was used; for CRRs with EC<sub>50</sub> values between 70 and 500 μM, a concentration of 3,160 or 10,000 μM was used; and for CRRs with EC<sub>50</sub> values >500 μM, a concentration of 10,000 μM was used. N/A, not applicable; No current, no GABA<sub>max</sub>-evoked peak-current amplitude exceeded 5 nA in any of the tested oocytes.

<sup>a</sup>Data were from n = 5 experiments performed on oocytes that had been incubated for 5–6 d following cRNA injection and selected based on GABA<sub>max</sub>-evoked current amplitudes; note that data for these n = 5 oocytes are not included in the number of oocytes tested or GABA<sub>max</sub> results.

<sup>b</sup>Given the GABA EC<sub>50</sub> value at this construct combination, the utilized 316-μM GABA<sub>max</sub> concentration represents a submaximal EC<sub>70–80</sub> concentration; an EC<sub>100</sub> concentration would thus be expected to give values that are 20–30% larger.

<sup>c</sup>Only 80–90% of the fitted curve is covered by data points (Fig. 9 C) and derived fitted values could therefore be seen as lower limits.

<sup>d</sup>These values are derived from first-order fitting; however, data are statistically better represented by second-order fitting as described in the text.

In summary, injection of cRNA for dimeric β-23-α or α-10-β constructs into oocytes either alone or in combination with free β2 or γ2 subunits led to expression of functional receptors in all cases. Based on the average current levels, there was no difference in how well the two constructs express. While data for the binary scenarios did not reveal specific information regarding assembly orientation, the ternary scenarios with free γ2 subunits showed that the dimers oriented themselves in opposite orientations. Finally, it is important to note that we only discussed and illustrated the simplest assembly scenarios and more complex scenarios cannot be excluded. These could include dimers or receptors with numerous dangling subunits, as suggested by Groot-Kormelink et al. (2004) for nAChRs.

#### Concatemers from tetrameric constructs based on α-10-β can assemble in both orientations

To further substantiate that concatemers with nonoptimal linker lengths can assemble in both orientations, we designed new tetrameric constructs. For reasons that will be explained below (“Design of new dimeric constructs” section), we were particularly interested in generating constructs with α1 as the first subunit. Two new constructs, α-10-β-α-β and α-10-β-α-γ, were made by extending the α-10-β construct using primarily AGS repeats for the new linkers. Note that these constructs differ by having a β2 or a γ2 subunit in the fourth construct position. To prevent new linkers in the constructs from negatively affecting assembly and/or function of the receptors formed, linkers longer than those in β-23-α and α-10-β dimers were used. Using our total-linker-length calculation

methodology, which is explained in the next section, the β-23-α and α-10-β constructs have “total linker lengths” ranging from 37 to 41 amino acids, and we chose to standardize on 45 amino acids for the new linkers (Table 3). An (AGS)<sub>5</sub>LGS(AGS)<sub>3</sub> linker was used to fuse the β2<sup>second</sup>-α1<sup>third</sup> subunit and consists of nine AGS repeats, where one repeat was altered from AGS to LGS to allow introduction of a unique restriction (HindIII) site. An AGT(AGS)<sub>5</sub> linker was used to fuse the α1<sup>third</sup>-β2<sup>fourth</sup> pair and consists of six AGS repeats with one repeat altered to AGT to allow a unique restriction (KpnI) site. An AGT linker consisting of one repeat was used to fuse the α1<sup>third</sup>-γ2<sup>fourth</sup> pair. Note that, although the specific linker sequences added to fuse these subunit pairs contained a different number of AGS repeats, the total linker length remains the same at 45 amino acids in all cases due to naturally occurring N- and C-terminal sequences (further explained in the next section).

Injection of cRNA for the tetrameric constructs alone resulted in GABA<sub>max</sub>-evoked peak-current amplitudes in the 60–150-nA range (Table 1). Hence, in agreement with observations for dimers, tetramers are also able to assemble into functional receptors by themselves, likely with three dangling subunits. To accomplish normal pentameric assembly, the tetrameric constructs were next coexpressed with a free γ2 or β2 subunit. As expected, α-10-β-α-β + γ2 and α-10-β-α-γ + β2 coinjections led to substantially larger and similar GABA<sub>max</sub>-evoked peak-current amplitudes in the ~5–7-μA range (Fig. 4 A). Full CRRs revealed fitted EC<sub>50</sub> values in the 32–34-μM range for GABA (Fig. 4, B and C) and in the 0.092–0.10-μM range for zolpidem (Fig. 4 D). These values are essentially identical to the values observed with

Table 2. Regression results from fitted zolpidem responses at wild-type and concatenated GABA<sub>A</sub>Rs

Construct	Subunit	Zolpidem			GABA <sub>316</sub> μM (nA)
		EC <sub>50</sub> (μM)	pEC <sub>50</sub>	n	
α1 + β2 1:50		No effect		7	2,100 ± 300
α1 + β2 50:1		No effect		6	750 ± 250
α1 + β2 + γ2 5:1:5		0.11	6.95 ± 0.02	11	2,900 ± 500
Dimeric constructs					
β2-23-α1	γ2	0.10	7.00 ± 0.03	8	7,600 ± 700
α1-10-β2	γ2	0.18	6.74 ± 0.03	7	14,000 ± 6,000
α1-9a-β2	γ2	0.19	6.72 ± 0.03	14	7,000 ± 1,000
α1-6a-β2	γ2	0.15	6.83 ± 0.03	8	4,000 ± 500
α1-3a-β2	γ2	0.20	6.71 ± 0.04	7	5,600 ± 1,300
α1-0a-β2	γ2	0.21	6.68 ± 0.03	12	280 ± 50
Tetrameric constructs					
α1-10-β2-α1-β2	γ2	0.10	7.00 ± 0.03	9	5,000 ± 500
α1-10-β2-α1-γ2	β2	0.092	7.04 ± 0.02	7	5,800 ± 400
Pentameric constructs					
α1-(-1a)-β2-α1-β2-γ2		0.17	6.76 ± 0.02	6	150 ± 50 <sup>a</sup>
α1-(-1a)-β2-α1-γ2-β2		0.19	6.72 ± 0.02	12	2,300 ± 300 <sup>a</sup>
γ2-15a-β2-α1-β2-α1		0.15	6.82 ± 0.02	9	6,100 ± 1,200
γ2-13a-β2-α1-β2-α1		0.22	6.65 ± 0.02	11	4,400 ± 600 <sup>a</sup>
γ2-11a-β2-α1-β2-α1		0.27	6.57 ± 0.03	12	2,000 ± 30 <sup>a</sup>
γ2-10a-β2-α1-β2-α1		0.14	6.86 ± 0.02	11	1,700 ± 200 <sup>a</sup>
γ2-9a-β2-α1-β2-α1		0.17	6.78 ± 0.03	14	800 ± 150 <sup>a</sup>
Mutant constructs					
α1-9a-β2	γ2(A118R)	3.4	5.46 ± 0.04	11	8,600 ± 1,100
α1-0a-β2	γ2(A118R)	2.0	5.70 ± 0.03	7	990 ± 90
α1 <sup>R94A</sup> + β2 + γ2 5:1:5		0.20	6.71 ± 0.02	7	990 ± 110 <sup>a</sup>
γ2-11a-β2-α1-β2-α1 <sup>R94A</sup>		0.36	6.44 ± 0.03	11	350 ± 50 <sup>a</sup>
γ2-11a-β2-α1-β2-α1 <sup>R94A</sup>	α1	0.20	6.71 ± 0.03	9	510 ± 130 <sup>a</sup>

Data points were fitted to the Hill equation with bottom set to 0 and Hill slope set to 1 by nonlinear regression. Fitted potencies of zolpidem are presented as EC<sub>50</sub> in μM and pEC<sub>50</sub> ± SEM where p = -Log for the indicated number (n) of individual oocytes. The average peak-current amplitudes obtained with GABA<sub>316</sub> μM applications are presented as mean ± SEM in nA for the tested oocytes. No effect, no positive enhancement of GABA<sub>control</sub>-evoked currents was observed.

<sup>a</sup>Due to the GABA EC<sub>50</sub> value on this receptor, GABA<sub>316</sub> μM applications do not represent a maximal EC<sub>100</sub> concentration.

free subunits in a biased ratio, suggesting that receptors based on linked tetramers resemble wild-type receptors.

Given the construct designs, only two simple (α1)<sub>2</sub>(β2)<sub>2</sub>(γ2) receptor stoichiometries can arise in each case. These have all linkers assembled in either the clockwise or the counterclockwise orientation (Fig. 4 E). However, in each case, only one of these possibilities results in the canonical receptor with two GABA-binding β2-α1 interfaces and a zolpidem-binding α1-γ2 interface (Fig. 4 E, two lower receptors). The other possibility gives a receptor with only one GABA-binding β2-α1 interface and no zolpidem-binding α1-γ2 interface (Fig. 4 E, two upper receptors). Therefore, functional receptors must be the result of assemblies with the linkers of the α-10-β-α-β concatemer in the clockwise

orientation and the α-10-β-α-γ concatemer in the counterclockwise orientation.

#### Definition of “total linker length” and shortest possible length predictions

As the N- and C-terminal ends differ considerably in their sequence and length among Cys-loop receptor subunits, there is a need for a consensus to calculate linker lengths. For this purpose, we used the method described by Ahring et al. (2018) in calculating linker lengths for concatenated nAChR constructs. The methodology establishes anchors based on conserved residues within the Cys-loop receptor family from which total linker sequences are calculated. The end of the transmembrane



Table 3. Total-linker-length calculations for concatenated GABA<sub>A</sub>R constructs

Subunit linking				Total-linker-length calculation					
Linked set	C-term.	Linker sequence	N-term.	End TM4	C-tail	Linker	N-term. to Anchor	Anchor	Sum
Dimeric constructs									
β2-23-α1	LYYVN	Q <sub>3</sub> (Q <sub>2</sub> A <sub>3</sub> PA) <sub>2</sub> AQ <sub>5</sub>	QPSLQ	WLYYV	1	23	17	ILDRL	41
α1-10-β2	PTPHQ	LQ <sub>9</sub>	QSVND	WATYL	13	10	14	TVDRL	37
α1-9a-β2	PTPHQ	(AGS) <sub>3</sub>	QSVND	WATYL	13	9	14	TVDRL	36
α1-6a-β2	PTPHQ	(AGS) <sub>2</sub>	QSVND	WATYL	13	6	14	TVDRL	33
α1-3a-β2	PTPHQ	AGS	QSVND	WATYL	13	3	14	TVDRL	30
α1-0a-β2	PTPHQ	AGS	NDPSN	WATYL	13	3	11	TVDRL	27
α1-(-1a)-β2	PTPHQ	AGS	DPSNM	WATYL	13	3	10	TVDRL	26
α1-(-2a)-β2	PTPHQ	AGS	PSNMS	WATYL	13	3	9	TVDRL	25
α1-(-3a)-β2	PTPHQ	AGS	SNMSL	WATYL	13	3	8	TVDRL	24
Tetrameric and pentameric constructs									
α1 <sup>first</sup> -10-β2 <sup>second</sup>	PTPHQ	LQ <sub>9</sub>	QSVND	WATYL	13	10	14	TVDRL	37
α1 <sup>first</sup> -(-1a)-β2 <sup>second</sup>	PTPHQ	AGS	DPSNM	WATYL	13	3	10	TVDRL	26
γ2 <sup>first</sup> -15a-β2 <sup>second</sup>	SYLYL	(AGS) <sub>5</sub>	QSVND	SYLYL	1	15	14	TVDRL	30
γ2 <sup>first</sup> -13a-β2 <sup>second</sup>	SYLYL	S(AGS) <sub>4</sub>	QSVND	SYLYL	1	13	14	TVDRL	28
γ2 <sup>first</sup> -11a-β2 <sup>second</sup>	SYLYL	GS(AGS) <sub>3</sub>	QSVND	SYLYL	1	11	14	TVDRL	26
γ2 <sup>first</sup> -10a-β2 <sup>second</sup>	SYLYL	S(AGS) <sub>3</sub>	QSVND	SYLYL	1	10	14	TVDRL	25
γ2 <sup>first</sup> -9a-β2 <sup>second</sup>	SYLYL	(AGS) <sub>3</sub>	QSVND	SYLYL	1	9	14	TVDRL	24
β2 <sup>second</sup> -α1 <sup>third</sup>	LYYVN	(AGS) <sub>5</sub> LGS(AGS) <sub>3</sub>	QPSLQ	WLYYV	1	27	17	ILDRL	45
α1 <sup>third</sup> -β2 <sup>fourth</sup>	PTPHQ	AGT(AGS) <sub>5</sub>	QSVND	WATYL	13	18	14	TVDRL	45
α1 <sup>third</sup> -γ2 <sup>fourth</sup>	PTPHQ	AGT	QKSDD	WATYL	13	3	29	ILNNL	45
β2 <sup>fourth</sup> -α1 <sup>fifth</sup>	LYYVN	(AGS) <sub>4</sub> ATG(AGS) <sub>4</sub>	QPSLQ	WLYYV	1	27	17	ILDRL	45
γ2 <sup>fourth</sup> -β2 <sup>fifth</sup>	SYLYL	(AGS) <sub>2</sub> ATG(AGS) <sub>5</sub>	QSVND	SYLYL	1	24	14	TVDRL	39

The five most proximal C-terminal amino acids (C-term.), the specific linker sequences introduced during concatenation (Linker sequence), and the five first amino acids from the predicted mature N terminus (N-term.) are presented for the indicated subunit pairs. Total-linker-lengths (Sum) are calculated as the sum of all existing amino acids and introduced linker sequence between two artificial fix points “End TM4” and “Anchor.” The five most proximal amino acids in TM4 (End TM4) and C-terminal tail lengths (C-tail) are obtained from UniProt (P14867 for α1 and P47870 for β2). The N-terminal lengths (N-term. to Anchor) are derived from a definition of an α-helix 1 anchor (Anchor) as described in the text. For tetrameric and pentameric constructs, numbers in superscript indicate the construct position of each subunit (e.g., β2<sup>second</sup>: β2 subunit in the second construct position).

segment 4 (TM4) of the first subunit and a hydrophobic residue in α-helix 1 of the second subunit are chosen as anchor points to represent the start and the end of the total linker, respectively (Fig. 5 A). Hence, the term total linker length covers existing C- (of the first subunit) and N-terminal (of the second subunit) sequences as well as the synthetic linker that connects both subunits.

When viewed from the top, the α-helix 1 motifs in a Cys-loop receptor point in a clockwise orientation and are locked in a fixed position by two hydrophobic patches (ILxxLL<sup>23</sup> in α1 and TVxxLL<sup>19</sup> in β2) entrenched in hydrophobic pockets (Fig. 5 B). Using the Ahring et al. (2018) methodology, the Ile<sup>18</sup> residue in the α1 subunit and the corresponding Thr<sup>14</sup> residue in the β2 subunit represent N-terminal anchors (Fig. 5 B and Table 3). Note that, in this context, GABA<sub>A</sub>R β subunits represent outliers in comparison with most mammalian Cys-loop receptor subunits. Instead of a hydrophobic leucine or isoleucine residue, β subunits have a threonine residue that is traditionally considered

hydrophilic. However, with the methyl group pointing toward the hydrophobic patch, it can still engage in hydrophobic contacts to help anchor the α-helix 1 motif (Fig. 5 B).

The directional nature of the α-helix 1 motifs causes the minimal required total linker length to differ between clockwise and counterclockwise assemblies, with the latter being the shortest. Predicted minimum lengths required to link the α1 TM4 Leu<sup>416</sup> anchor to the β2 Thr<sup>14</sup> anchor were obtained based on modeling of the α1-β2 and β2-α1 subunit interfaces (Fig. 5 C). In the “short” counterclockwise orientation, a span of minimally 27 amino acids was required, whereas the “long” clockwise direction required minimally 30 amino acids (Fig. 5 C). Addition of fewer amino acids resulted in visual distortion of the α1 TM4 segment and/or the β2 helix 1 following a short geometry optimization indicative of a too short and constrained linker. Thus, the shortest possible counterclockwise linker is predicted to require three amino acids less than the shortest

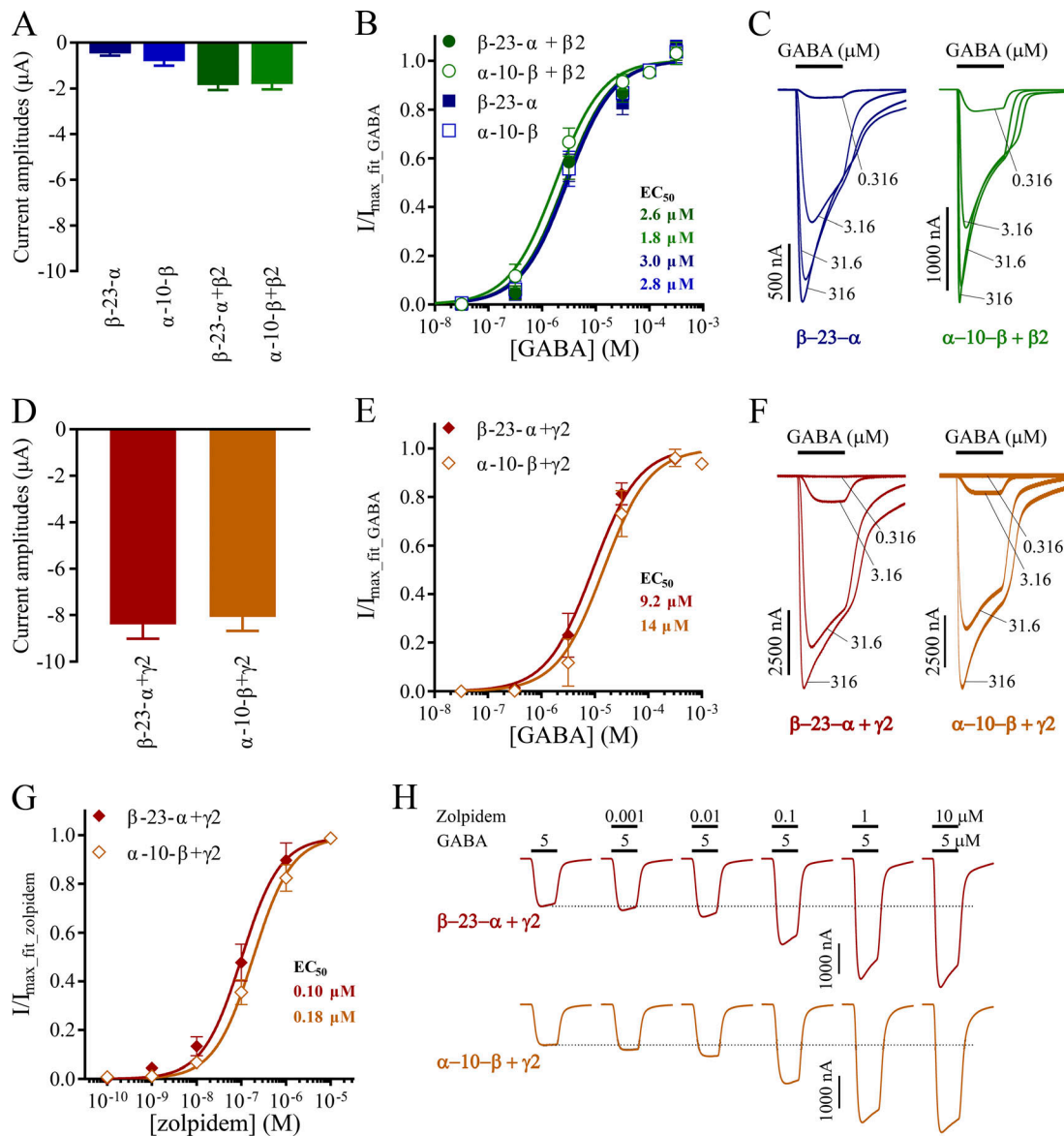


Figure 2. **Potency of GABA and zolpidem at GABA<sub>A</sub>Rs from concatenated  $\beta$ -23- $\alpha$  or  $\alpha$ -10- $\beta$  constructs.** *X. laevis* oocytes were subjected to two-electrode voltage-clamp electrophysiology and electrophysiological data were evaluated as described in the Materials and methods; also see Fig. 1. cRNA for  $\beta$ -23- $\alpha$  or  $\alpha$ -10- $\beta$  was injected alone (A, B, and C), coinjected with a free  $\beta$ 2 subunit in a 1:1 ratio (A, B, and C), or coinjected with a free  $\gamma$ 2 subunit in a 1:1 ratio (D, E, and F). (A and D) GABA<sub>max</sub>-evoked peak-current amplitudes are depicted as means  $\pm$  SEM for receptors from the indicated cRNA mixtures. A GABA concentration of 316  $\mu$ M was used as GABA<sub>max</sub>. Data were obtained from  $n = 8$ –13 experiments and calculated averages are presented in Table 1. (B and E) GABA CRRs are depicted as means  $\pm$  SD for receptors from the indicated cRNA mixtures. Data were obtained from  $n = 8$ –13 experiments and regression results are presented in Table 1. (C and F) Representative traces illustrating GABA CRRs at receptors from the indicated cRNA mixtures. Bars above the traces designate the 30-s application time and concentrations of applied GABA. (G) Zolpidem enhancement CRRs are depicted as means  $\pm$  SD for receptors from  $\beta$ -23- $\alpha + \gamma$ 2 or  $\alpha$ -10- $\beta + \gamma$ 2 coinjections. Datasets from each oocyte were normalized to the maximal fitted response to enhance visual comparison of EC<sub>50</sub> values. Data were from  $n = 7$ –8 experiments and regression results are presented in Table 2. (H) Representative traces illustrating zolpidem CRRs from G. Bars above the traces designate the 30-s application time and concentrations of applied GABA and zolpidem.

possible clockwise linker, which corresponds to  $\sim 10$  Å in distance difference.

### Design of new dimeric constructs

The aim for designing new linked dimeric constructs is to identify a potential linker length for which functional receptors only originate from counterclockwise assembly of dimers. As detailed in Ahring et al. (2018), short counterclockwise linkers

can be expected to pack tightly along the extracellular domain of, in particular, the first subunit of a linked dimer (Fig. 5 C). In cases where a linker packs tightly over the C-loop of a GABA-binding interface this could be envisioned to affect normal function. As  $\beta$ 2- $\alpha$ 1 dimers are more likely to be affected by this, we chose to work with  $\alpha$ 1- $\beta$ 2 constructs. Furthermore, we decided to use AGS-repeat linkers instead of poly-Q linkers. This strategy was successful for nicotinic  $\alpha$ 4 $\beta$ 2 receptors and is easily

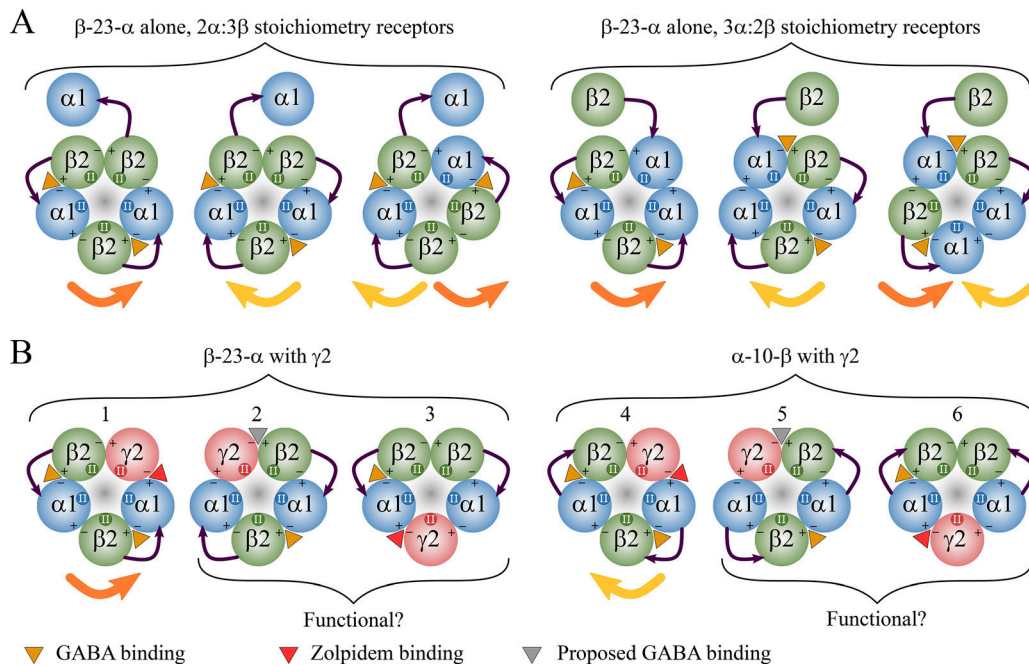


**Figure 3. Possible GABA<sub>A</sub>R assemblies with concatenated  $\beta$ -23- $\alpha$  or  $\alpha$ -10- $\beta$  constructs.**  $\beta$ 2,  $\alpha$ 1, and  $\gamma$ 2 subunits are illustrated as green, blue, and red circles, respectively, viewed from the extracellular space. The pore-lining transmembrane helix 2 domain is indicated by circles embedding the symbol "H". Principal and complementary subunit faces are indicated with "+" and "-", respectively. Linkers are shown as purple arrows progressing from the C terminus of the first subunit to the N terminus of the second. Linker orientation(s) within a receptor complex deemed functional is indicated underneath each receptor by orange (counterclockwise) or yellow (clockwise) arrows. Given no confirmed knowledge regarding the assembly orientation of linked  $\beta$ -23- $\alpha$  or  $\alpha$ -10- $\beta$  dimers, numerous possible assemblies can be envisaged depending on the specific cRNA content. Note that only the simplest possibilities are illustrated; more complex assemblies including di-pentamers or additional dangling subunits cannot be excluded. **(A)** Injection of the  $\beta$ -23- $\alpha$  or the  $\alpha$ -10- $\beta$  construct alone could lead to a receptor pool containing from one to six different receptor assemblies. These receptors can be of both 2 $\alpha$ :3 $\beta$  or 3 $\alpha$ :2 $\beta$  stoichiometries and have a dangling  $\alpha$ 1 or  $\beta$ 2 subunit. Only the  $\beta$ -23- $\alpha$  case is illustrated; however,  $\alpha$ -10- $\beta$  would give a fully similar scenario. **(B)** Coinjection of  $\beta$ -23- $\alpha$  +  $\gamma$ 2 or  $\alpha$ -10- $\beta$  +  $\gamma$ 2 could lead to a receptor pool containing from one to three different receptors in each case. However, for each construct, only one of these assembly possibilities results in a receptor with two canonical GABA-binding  $\beta$ 2- $\alpha$ 1 interfaces and a zolpidem-binding  $\alpha$ 1- $\gamma$ 2 interface (receptors 1 and 4). It is questionable whether the other assembly possibilities are functional, although one assembly has a single canonical GABA-binding  $\beta$ 2- $\alpha$ 1 interface and a proposed GABA-binding  $\beta$ 2- $\gamma$ 2 interface (receptors 2 and 5).

amenable for systematic shortening of the linker length and less likely to deplete specific tRNAs than a poly-Q linker.

The  $\beta$ -23- $\alpha$  construct has a total linker length of 41 amino acids, whereas the  $\alpha$ -10- $\beta$  construct has 37 amino acids (Fig. 5 A and Table 3). Initially, five new dimeric  $\alpha$ 1- $\alpha$ - $\beta$ 2 constructs with total linker lengths of 36, 33, 30, 27, and 24 amino acids were created. These were termed  $\alpha$ -9a- $\beta$ ,  $\alpha$ -6a- $\beta$ ,  $\alpha$ -3a- $\beta$ ,  $\alpha$ -0a- $\beta$ , and  $\alpha$ -(-3a)- $\beta$ , respectively. The nomenclature indicates how many amino acids (a) are added or removed to link the two sequences. For restriction site purposes, a minimum of one AGS repeat was introduced in all cases. Thus, in order to create the two shortest constructs, it was necessary to omit three and six existing amino acids, respectively, during the linking process. As the predicted mature GABA<sub>A</sub>R subunits generally have long N-terminal sequences upstream from the  $\alpha$ -helix 1 anchor, when compared with, for example, nAChR subunits, we chose to omit these amino acids from the  $\beta$ 2 N terminus (QSV and QSVNDP, respectively; Table 3).

### Shortened linker can lead to primarily counterclockwise assembly of dimeric concatemers

With a construct that is restricted to the shorter counterclockwise assembly, coexpression with  $\beta$ 2 should lead to fully functional  $\alpha$ 1 $\beta$ 2 receptors, whereas coexpression with  $\gamma$ 2 should lead

to receptors with only one GABA-binding  $\beta$ 2- $\alpha$ 1 interface (Fig. 3 B, receptor 5).

### $\alpha$ - $\alpha$ - $\beta$ alone

Average GABA<sub>max</sub>-evoked peak-current amplitudes decreased noticeably as the linker length was shortened (Fig. 6 A and Table 1). No single oocyte exhibited current amplitudes exceeding 5 nA with the shortest (-3a)-linked construct. While GABA-evoked currents were observed with the 0a-linked construct, the amplitudes were deemed insufficient for performing reliable GABA CRRs. For the remaining three constructs, GABA gave rise to CRRs with EC<sub>50</sub> values in the 3.2–10- $\mu$ M range (Fig. 6 B and Table 1). The lowest potency was observed with the shortest 3a-linked construct. No apparent differences were observed when comparing current traces from injections of  $\alpha$ -9a- $\beta$  and  $\alpha$ -3a- $\beta$  cRNA (Fig. 6 C).

### $\alpha$ - $\alpha$ - $\beta$ + $\beta$ 2

Inclusion of free  $\beta$ 2 subunits in the cRNA mixture led to robust GABA<sub>max</sub>-evoked peak-current amplitudes in most cases (Fig. 6 D and Table 1). Although maximal current amplitudes were only in the 40-nA range with the (-3a)-linked construct, this was sufficient to perform full CRR experiments. All fitted

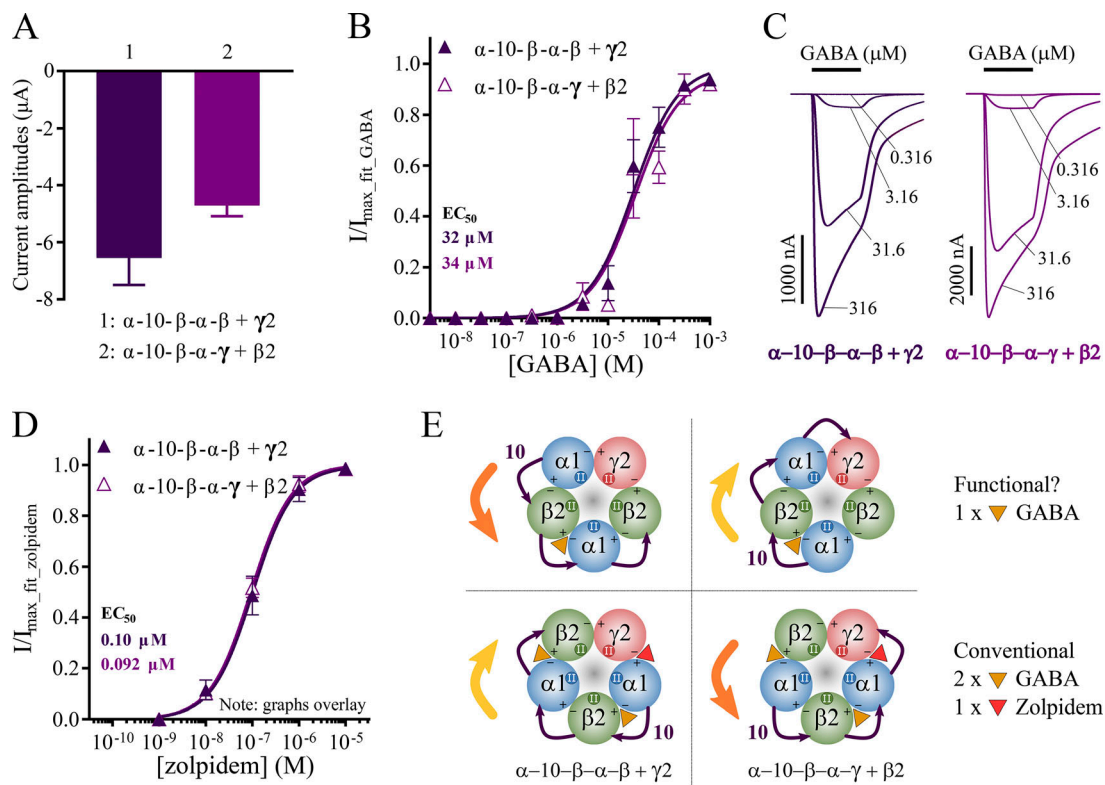


**Figure 4. Potency of GABA and zolpidem at GABA<sub>A</sub>Rs from concatenated tetrameric constructs based on the  $\alpha$ -10- $\beta$  construct.** *X. laevis* oocytes were injected with cRNA mixtures for  $\alpha$ -10- $\beta$ - $\alpha$ - $\beta$  +  $\gamma$ 2 or  $\alpha$ -10- $\beta$ - $\alpha$ - $\gamma$  +  $\beta$ 2 and subjected to two-electrode voltage-clamp electrophysiology. Electrophysiological data were evaluated as described in the Materials and methods; also see Fig. 1 and Fig. 2. **(A)** GABA<sub>max</sub>-evoked peak-current amplitudes are depicted as means  $\pm$  SEM for receptors from the indicated cRNA mixtures. A GABA concentration of 316  $\mu$ M was used as GABA<sub>max</sub>. Data were obtained from  $n = 9$ –11 experiments and calculated averages are presented in Table 1. **(B)** GABA CRRs are depicted as means  $\pm$  SD for receptors from the indicated cRNA mixtures. Data were obtained from  $n = 9$ –11 experiments and regression results are presented in Table 1. **(C)** Representative traces illustrating GABA CRRs at receptors from the indicated cRNA mixtures. Bars above the traces designate the 30-s application time, and concentrations of applied GABA are indicated for each trace. **(D)** Zolpidem enhancement CRRs are depicted as means  $\pm$  SD for the indicated receptors. Data were from  $n = 7$ –9 experiments and regression results are presented in Table 2. **(E)** Simplest potential receptor assemblies arising from injection of the tetrameric constructs with a free subunit. As the linked subunits might assemble in either the clockwise or the counterclockwise orientation, each case leads to two different assemblies. Of these, however, only one give receptors with two canonical GABA-binding  $\beta$ 2- $\alpha$ 1 interfaces and a zolpidem-binding  $\alpha$ 1- $\gamma$ 2 interface (lower panels).

$EC_{50}$  values for GABA CRRs were in the 1.7–4- $\mu$ M range (Fig. 6 E and Table 1). This is essentially identical to the 2.6  $\mu$ M obtained with receptors expressed with free subunits in a biased ratio (Fig. 1 A). Despite the current amplitude differences, no other visual difference was noted between current traces from  $\alpha$ -9a- $\beta$  +  $\beta$ 2 and  $\alpha$ -(-3a)- $\beta$  +  $\beta$ 2 injections (Fig. 6 F).

#### $\alpha$ -xa- $\beta$ + $\gamma$ 2

With construct linkers of 9a to 3a, GABA<sub>max</sub>-evoked peak-current amplitudes were substantial in the 3–11- $\mu$ A range when free  $\gamma$ 2 subunits were included in the cRNA mixture (Fig. 6 G and Table 1). The GABA CRRs revealed normal  $EC_{50}$  values in the 17–41- $\mu$ M range for these receptors (Fig. 6 H and Table 1). However, with the shorter 0a-linked construct, current amplitudes dropped substantially to 0.5  $\mu$ A, and interestingly this was accompanied by a lower GABA potency of 130  $\mu$ M. Despite this change, no obvious visual differences were noted between traces for  $\alpha$ -9a- $\beta$  +  $\gamma$ 2 and  $\alpha$ -0a- $\beta$  +  $\gamma$ 2 cRNA (Fig. 6 I). The average current amplitude was marginal at  $\sim$ 2 nA for  $n = 24$  oocytes with the shortest (-3a)-linked construct, which is, in general, too low for performing full CRR experiments (Table 1).

Clear GABA-evoked currents ranging from 2–4 nA were, however, observed in eight oocytes and a further two oocytes displayed amplitudes in the 5–22-nA range.

With respect to the aim of discovering a linker length that only allows dimers to assemble in the counterclockwise orientation, this appeared to be achieved with the  $\alpha$ -(-3a)- $\beta$  construct. Yet, this exclusivity came at a cost of a substantial loss in peak-current amplitudes when the construct was coexpressed with free  $\beta$ 2 subunits. Besides rendering the  $\alpha$ -(-3a)- $\beta$  construct useless for most practical purposes, the current amplitude loss also raises questions regarding receptor stoichiometry. Although restricted from clockwise assembly, a construct with the optimal total-linker-length should still express efficiently in the counterclockwise orientation. Hence, the amplitude loss could suggest that the observed currents are not solely from receptors assembled in a simple scenario with two dimers and a free  $\beta$ 2 subunit; receptors might instead be a mixture of complex scenarios where 2–3 free  $\beta$ 2 subunits assemble with dimers, such that linked  $\beta$ 2 subunits end up dangling. Complex dimer assembly scenarios of this kind were observed by Groot-Kormelink et al. (2004) for nAChRs. The next-shortest  $\alpha$ -0a- $\beta$



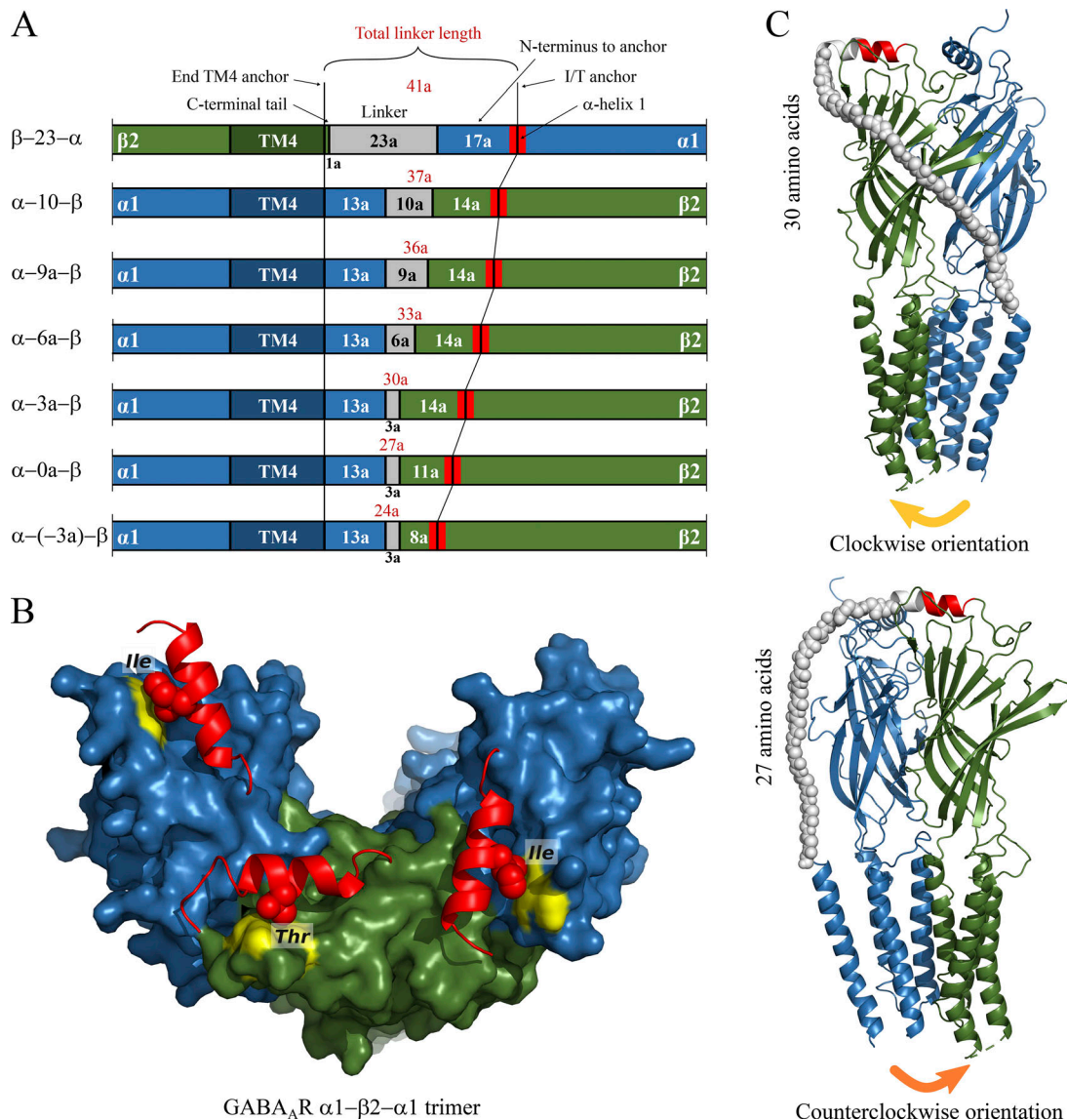


**Figure 5. Total linker calculations and 3-D structures of GABA<sub>A</sub>R interfaces.** Total-linker-length calculations are based on a methodology developed in [Ahring et al. \(2018\)](#). Besides added artificial linker sequences, C-terminal amino acids following the last residue in TM4 as well as N-terminal amino acids preceding a hydrophobic anchor (I/T anchor) in α-helix 1 are also considered parts of the linker. **(A)** The β-23-α and the α-10-β constructs originally designed by [Baumann et al. \(2001\)](#) have total linker lengths of 41 and 37 amino acids, respectively. Below these constructs, calculations for new concatenated α-x-β dimer constructs are illustrated. Note that only partial cDNA sequences in the vicinity of the linkers is shown. **(B)** Top view of α1-β2-α1 trimer interfaces highlighting the N-terminal α-helix 1 motifs. When viewed from the top, the helix motifs are pointing in a clockwise orientation. The α1 subunit is colored green, β2 is blue, the α-helix 1 is red, anchor Ile/Thr residues are shown as red spheres, and hydrophobic areas within 4 Å of the anchors are colored yellow. **(C)** α1-β2 dimer with modeled long clockwise and short counterclockwise linkers. The backbone of the linker is shown in white space-filling representation. The least number of amino acids required to connect the last α1 residue in TM4 (Leu<sup>443</sup>) to the mature N terminus of β2 (Glu<sup>25</sup>) was 13 and 16 residues, respectively. This corresponds to a total linker length of 27 and 30 residues (white) as calculated between anchors α1 Leu<sup>443</sup> and β2 Thr<sup>39</sup> ([Table 3](#)).

construct resulted in overall similar current amplitudes when coexpressed with free β2 or γ2 subunits. To investigate whether intermediate linker lengths would be superior, two additional constructs termed α-(-1a)-β and α-(-2a)-β were created, which have total linker lengths of 26 and 25 amino acids, respectively.

#### α-(-1a)-β and α-(-2a)-β

No GABA<sub>max</sub>-evoked peak-current amplitudes exceeding 5 nA were observed with the (-1a)- and (-2a)-linked constructs

injected by themselves ([Fig. 6 J](#)). In contrast, coexpression with free β2 subunits resulted in robust current amplitudes in the 400-nA range. The fitted EC<sub>50</sub> value for the GABA CRR was 2.6 μM for both constructs ([Fig. 6, K and L](#)). When coexpressed with free γ2 subunits, average current amplitudes of ~8 nA were observed ([Table 1](#)). While this is overall too low for obtaining GABA CRRs, current amplitudes in the 20–50-nA range were observed in 5–10% of the oocytes.

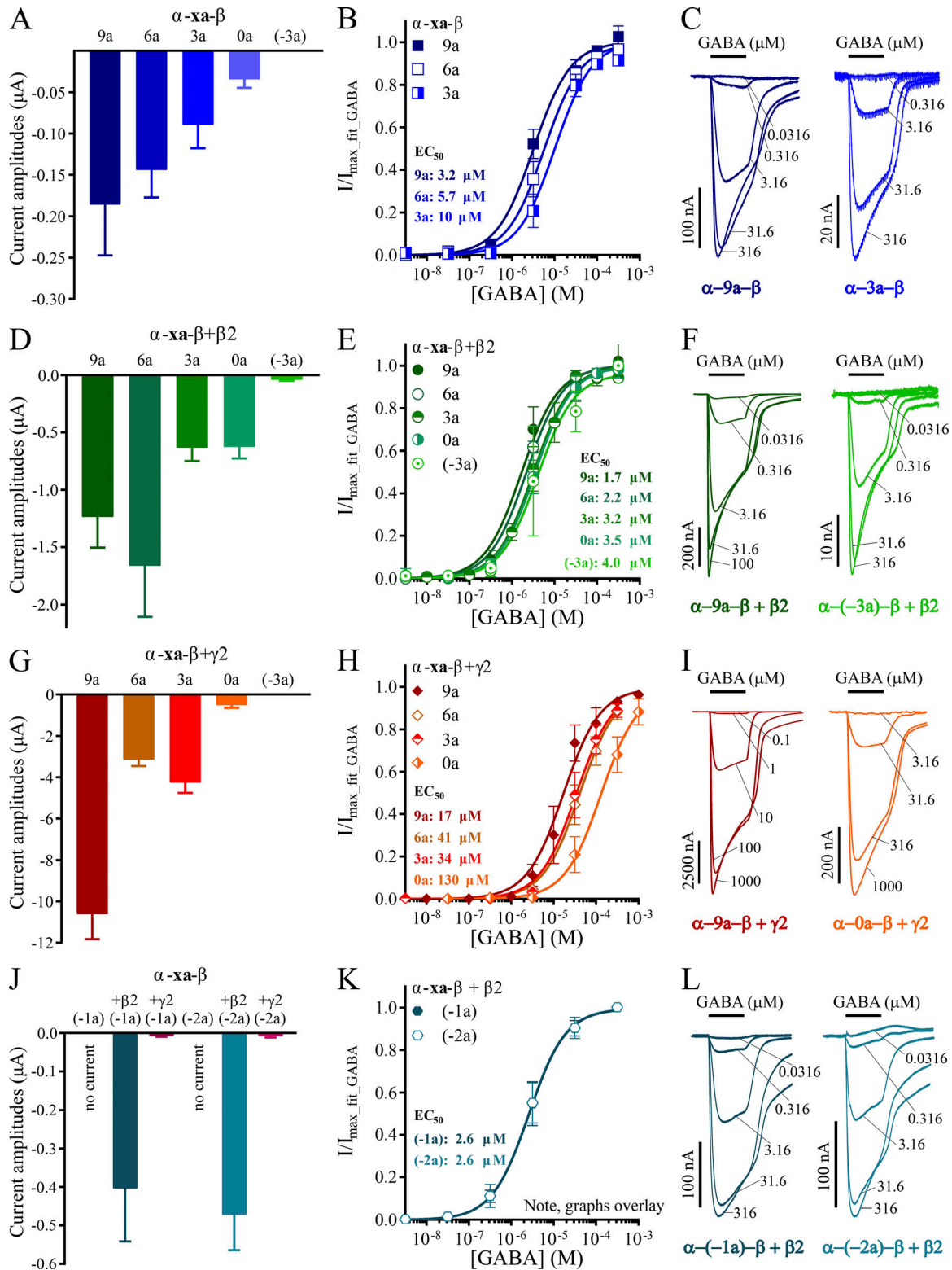


Figure 6. **GABA potency at GABA<sub>A</sub>Rs from concatenated  $\alpha$ -xa- $\beta$  dimer constructs.** *X. laevis* oocytes were subjected to two-electrode voltage-clamp electrophysiology and electrophysiological data were evaluated as described in the Materials and methods; also see Fig. 1. cRNA for  $\alpha$ -xa- $\beta$  constructs were injected alone (A, B, C, and J), coinjected with a monomeric  $\beta$ 2 subunit in a 1:1 ratio (D, E, F, J, K, and L), or coinjected with a monomeric  $\gamma$ 2 subunit in a 1:1 ratio (G, H, I, and J). **(A, D, G, and J)** GABA<sub>max</sub>-evoked peak-current amplitudes are depicted as means  $\pm$  SEM for receptors from the indicated cRNA mixtures. A GABA concentration of 316  $\mu$ M was used as GABA<sub>max</sub> for all construct combinations with the exception of  $\alpha$ -10- $\beta$ + $\gamma$ 2, for which a concentration of 3,160  $\mu$ M was used. Data were obtained from  $n = 7$ –24 experiments and calculated averages are presented in Table 1. **(B, E, H, and K)** GABA CRRs are depicted as means  $\pm$  SD for receptors from the indicated cRNA mixtures. Data were obtained from  $n = 7$ –24 experiments and regression results are presented in Table 1. **(C, F, I, and L)** Representative traces illustrating GABA CRRs at receptors from the indicated cRNA mixtures. Bars above the traces designate the 30-s application time and concentrations of applied GABA are indicated for each trace.

### GABA CRRs for (-1a)-, (-2a)-, and (-3a)-linked constructs coexpressed with $\gamma 2$

When coexpressed with free  $\gamma 2$  subunits, the three shortest constructs all resulted in low average current amplitudes, yet some oocytes still expressed robustly. Since the GABA  $EC_{50}$  value for the 0a-linked construct is 130  $\mu M$ , it could be speculated that the  $EC_{50}$  values for the three shorter constructs are further shifted toward lower potency, which might exclude functional receptors from being detected by a GABA $_{max}$  concentration of 316  $\mu M$ . In an attempt to obtain GABA CRRs for these construct combinations, a separate set of experiments was performed using oocytes incubated for 5–6 d following injection and selection of those that displayed GABA $_{max}$ -evoked peak-current amplitudes exceeding 20 nA. For each combination, a total of  $n = 5$  oocytes were identified and these had average current amplitudes evoked by 10 mM GABA in the 53–100-nA range, with the lowest value observed for the (-3a)-linked construct. GABA  $EC_{50}$  values for the three combinations were in the range of 64–140  $\mu M$ , with the most potent value observed for the (-3a)-linked construct (Table 1). Given the overall low current amplitudes, these values appear similar and match that observed with the (0a)-linked construct. While these data show that the three constructs coexpressed with  $\gamma 2$  can give functional receptors, it is important to note that these separate experiments required substantial oocyte selection, in particular for the (-3a)-linked construct.

Overall, the picture with the new dimers is one where usage of shorter linkers increases control of concatemer assembly. Whereas the linker in the (0a)-linked construct is long enough to allow some assembly with the  $\gamma 2$  subunit in the clockwise orientation, the one in the (-3a)-linked construct is too short even for efficient counterclockwise assembly with the  $\beta 2$  subunit. In between, the (-1a)- and (-2a)-linked constructs express efficiently and consistently in the counterclockwise orientation with free  $\beta 2$  subunits but not in the clockwise orientation with free  $\gamma 2$  subunits. Hence, a total-linker-length of 25–26 amino acids appears suited for ensuring that functional receptors based on dimeric  $\alpha 1$ - $\alpha$ - $\beta 2$  constructs originate from linkers assembled primarily in the counterclockwise orientation.

### Why does the GABA $EC_{50}$ value differ between the dimeric constructs coexpressed with $\gamma 2$ ?

Whereas coexpression experiments of  $\alpha 1$ - $\alpha$ - $\beta 2$  dimeric constructs with free  $\beta 2$  subunits gave essentially identical GABA  $EC_{50}$  values, irrespective of linker length, corresponding experiments with free  $\gamma 2$  subunits revealed a noticeable shift between constructs with short versus long linkers. An  $EC_{50}$  value of 130  $\mu M$  was observed for the 0a-linked constructs, whereas values in the 17–41- $\mu M$  range were observed for longer linked constructs (Fig. 6 H and Table 1). Given the ability of dimers with long linkers to assemble into  $\alpha 1\beta 2$  receptors by themselves, it appears likely that the  $EC_{50}$  value for, for example, the  $\alpha 1$ -9a- $\beta 2$  construct is influenced by pollutant  $\alpha 1\beta 2$  receptors. Still, the approximately fourfold  $EC_{50}$ -value difference between the  $\alpha 1$ -3a- $\beta 2$  and the  $\alpha 1$ -0a- $\beta 2$  constructs coexpressed with  $\gamma 2$  appears intriguing. Obviously, this could simply be a secondary effect of short linkers since linked dimers must orient themselves in the

unfavorable long clockwise orientation to yield receptors in the canonical  $\beta\alpha\beta\alpha\gamma$  assembly (Fig. 3 B, receptor 4). However, another intriguing explanation could be that  $\alpha 1$ -0a- $\beta 2 + \gamma 2$  leads to receptors with an alternative subunit arrangement. It was previously proposed that  $\beta\gamma$  receptors express functionally and respond to GABA in the micromolar range (Whittemore et al., 1996; Chua et al., 2015; Wongsamitkul et al., 2017). Hence, if the linked  $\alpha 1$ -0a- $\beta 2$  dimers orient themselves in the shortest counterclockwise orientation, the  $\gamma 2$  subunit would be positioned alternatively in a  $\beta\alpha\beta\gamma\alpha$  assembly (Fig. 3 B, receptor 5). Assuming that two agonist GABA-binding sites are necessary for receptor activation, the  $EC_{50}$  value shift could then be the result of lower GABA potency at the  $\beta 2$ - $\gamma 2$  interface.

To differentiate between these two possibilities, GABA and zolpidem CRRs were compared at receptors from 9a- and 0a-linked constructs coexpressed with either a wild-type  $\gamma 2$  or a mutant  $\gamma 2^{A79R}$  subunit. The  $\gamma 2^{A79}$  loop D residue is centrally placed on the complementary side in the benzodiazepine  $\alpha 1$ - $\gamma 2$  binding pocket and corresponds to an important GABA-binding arginine,  $\alpha 1^{R67}$ , in the  $\beta 2$ - $\alpha 1$  interface (Bergmann et al., 2013). Thus, if receptors are of the canonical  $\beta\alpha\beta\alpha\gamma$  stoichiometry (i.e., with dimers assembled in the long clockwise orientation) the mutation should negatively affect the potency of zolpidem in the  $\alpha 1$ - $\gamma 2^{A79R}$  interface. However, if receptors are of the alternative  $\beta\alpha\beta\gamma\alpha$  stoichiometry (i.e., with dimers assembled in the short counterclockwise orientation) the mutation should increase the potency of GABA in the  $\beta 2$ - $\gamma 2^{A79R}$  interface. Interestingly, the results from these experiments were clear cut. Whereby the potency of GABA was affected by linker length, it was not affected by the A79R mutation in  $\gamma 2$  (Fig. 7 A and Table 1). In contrast, the potency of zolpidem was not affected by linker length but decreased by  $\sim 10$ -fold with the  $\gamma 2^{A79R}$  subunit mutation (Fig. 7 B and Table 2). This demonstrates that receptors have the canonical  $\beta\alpha\beta\alpha\gamma$  stoichiometry in both cases.

The data exclude  $\beta 2$ - $\gamma 2$  interfaces as the cause for the arguably small  $EC_{50}$  value shift between the 3a- and 0a-linked constructs. Moreover, the marginal current amplitudes observed for the (-1a)- and (-2a)-linked constructs coexpressed with free  $\gamma 2$  subunits in the previous section corroborate the notion that  $\beta 2$ - $\gamma 2$  interfaces are not significantly contributing to receptor activation for these constructs either. Hence, the most likely explanation for the shift is secondary effects from inclusion of short linkers; however, what this exactly constitutes remains elusive. One possibility is that short linkers in the unfavorable clockwise orientation cause tighter packing of the total receptor complex. Another possibility is that the passage of short clockwise linkers across GABA-binding interfaces alters the mobility of the  $\beta 2$  C-loop. While less likely, it also remains possible that functional receptors from the 0a-linked construct contain more than two dimers with associated interfering dangling subunits.

### Using one short linker to force counterclockwise orientation of pentameric concatemers

To evaluate whether a short first linker can force pentameric concatemers to assemble with their linkers predominantly in the counterclockwise orientation, two new constructs,  $\alpha$ -(-1a)- $\beta$ - $\alpha$ - $\beta$ - $\gamma$  and  $\alpha$ -(-1a)- $\beta$ - $\alpha$ - $\gamma$ - $\beta$ , were made by extending the  $\alpha$ -(-1a)- $\beta$



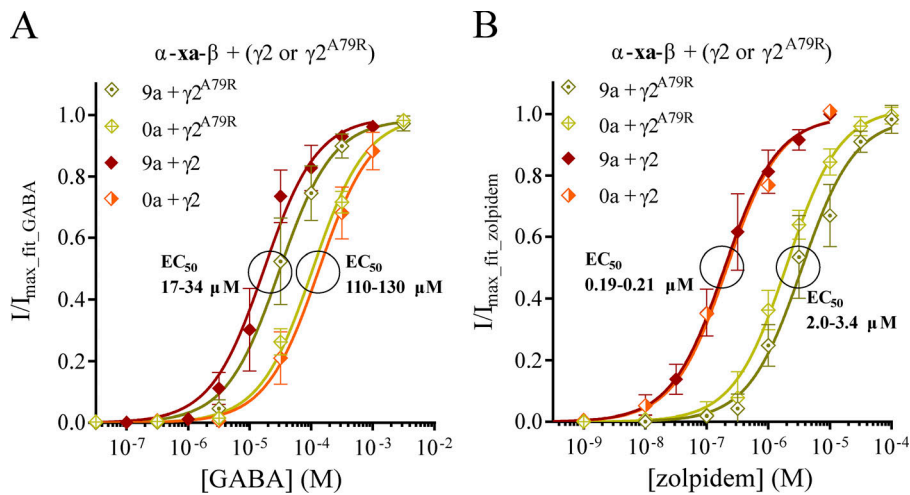


**Figure 7. GABA and zolpidem potency at wild-type or mutant concatenated GABA<sub>A</sub>Rs.** *X. laevis* oocytes were subjected to two-electrode voltage-clamp electrophysiology and electrophysiological data were evaluated as described in the Materials and methods; also see Fig. 1. cRNA for dimeric  $\alpha$ -9a- $\beta$  or  $\alpha$ -0a- $\beta$  constructs were mixed with cRNA for the wild-type  $\gamma$ 2 or mutant  $\gamma$ 2<sup>A79R</sup> subunit in a 1:1 ratio. **(A)** GABA CRRs are depicted means  $\pm$  SD for receptors from the indicated cRNA mixtures. Data were obtained from  $n = 9$ –20 experiments and regression results are presented in Table 1. **(B)** Zolpidem enhancement CRRs are depicted as means  $\pm$  SD for the indicated receptors. Data were from  $n = 7$ –14 experiments and regression results are presented in Table 2.

construct (Table 3). Note, that these constructs vary primarily by the positions of the last two subunits. The linker sequences introduced to fuse the  $\beta$ 2<sup>second</sup>- $\alpha$ 1<sup>third</sup>,  $\alpha$ 1<sup>third</sup>- $\beta$ 2<sup>fourth</sup>, or  $\alpha$ 1<sup>third</sup>- $\gamma$ 2<sup>fourth</sup> subunit pairs were identical to those used for the tetrameric constructs above. An (AGS)<sub>4</sub>ATG(AGS)<sub>4</sub> linker was used for the  $\beta$ 2<sup>fourth</sup>- $\alpha$ 1<sup>fifth</sup> pair and consisted of 27 amino acids, which essentially can be subdivided into nine AGS repeats with one repeat altered from AGS to ATG to allow introduction of a unique restriction (AgeI) site (Table 3). Fusion of the  $\gamma$ 2<sup>fourth</sup>- $\beta$ 2<sup>fifth</sup> subunit pair was obtained with a similar but one repeat shorter (AGS)<sub>2</sub>ATG(AGS)<sub>5</sub> linker. Although that results in a total linker length of 39 instead of the standard 45 amino acids, this still appears substantially longer than minimally needed.

Whereas injection of both constructs gave rise to GABA-evoked currents, the maximal current amplitude levels differed substantially (Fig. 8 A and Table 1). With average amplitudes of 320 nA for  $\alpha$ -(-1a)- $\beta$ - $\alpha$ - $\beta$ - $\gamma$  and 3,500 nA for  $\alpha$ -(-1a)- $\beta$ - $\alpha$ - $\gamma$ - $\beta$  the difference was  $\sim$ 11-fold; however, this underestimates the actual difference between randomly chosen oocytes, as  $\sim$ 25% of the oocytes for  $\alpha$ -(-1a)- $\beta$ - $\alpha$ - $\beta$ - $\gamma$  were discarded due to low GABA<sub>max</sub>-evoked peak-current amplitudes. The GABA and zolpidem CRRs revealed similar fitted  $EC_{50}$  values in the 330–390- $\mu$ M and 0.17–0.19- $\mu$ M ranges, respectively (Fig. 8, B–D; Table 1; and Table 2). This demonstrates that efficient expression of functional receptors only occurs with the concatemers in a counterclockwise assembly once the first construct linker is short (Fig. 8 E). That said, the  $\sim$ 10-fold lower GABA potency at both pentamers in comparison with, for example, data for tetramers was a surprising observation (Table 1).

### Optimizing the design of pentameric constructs

Why the  $\alpha$ -(-1a)- $\beta$ - $\alpha$ - $\gamma$ - $\beta$  construct resulted in a notably shifted GABA  $EC_{50}$  value of 330  $\mu$ M when the concatemer has the ability to assemble efficiently in the optimal counterclockwise orientation is unclear. We speculate that the reason for this might be a complex combination of a short first linker and the specific position of the  $\gamma$ 2 subunit within the construct. Possibly, it is generally unfavorable to have the  $\gamma$ 2 subunit linked in both its N

and C termini. To investigate this, we created a set of new pentameric constructs in which the  $\gamma$ 2 subunit was only linked at the C terminus. These were termed  $\gamma$ -xa- $\beta$ - $\alpha$ - $\beta$ - $\alpha$  and have a first AGS-repeat-based linker addition of  $x = 15, 13, 11, 10,$  or 9 amino acids, which correspond to total linker lengths of 30, 28, 26, 25, and 24 amino acids, respectively (Fig. 9 A and Table 3). Note that these total linker lengths correspond to dimeric constructs ranging from  $\alpha$ -3a- $\beta$  (30 amino acids) to  $\alpha$ -(-3a)- $\beta$  (24 amino acids). The linker sequences used to fuse the  $\beta$ 2<sup>second</sup>- $\alpha$ 1<sup>third</sup>,  $\alpha$ 1<sup>third</sup>- $\beta$ 2<sup>fourth</sup>, and  $\beta$ 2<sup>fourth</sup>- $\alpha$ 1<sup>fifth</sup> subunit pairs were identical to those for the pentameric constructs above. When assembled in the counterclockwise orientation, these new concatemers all yield the canonical  $\beta\alpha\beta\alpha\gamma$  receptor.

While injections of 15a-, 13a-, 11a-, and 10a-linked constructs gave rise to maximal GABA-evoked current amplitudes in the 3.1–5.3- $\mu$ A range, the shortest 9a-linked construct displayed lower current amplitudes of 0.89  $\mu$ A (Table 1). GABA CRRs revealed  $EC_{50}$  values in the 51–120- $\mu$ M range (Fig. 9 B and Table 1). This is similar to the 70–80- $\mu$ M values observed previously with a pentameric construct or mixtures of dimeric and trimeric constructs (Baur et al., 2006; Söderhielm et al., 2018). Zolpidem displayed essentially identical CRRs with  $EC_{50}$  values in the 0.14–0.27- $\mu$ M range, thereby mimicking that observed for free subunits in a biased ratio (Table 2).

While the data do suggest that shortening of the first linker in a  $\gamma$ -xa- $\beta$ - $\alpha$ - $\beta$ - $\alpha$  construct can have a secondary effect on GABA potency, the  $EC_{50}$  values obtained with these constructs are all within a narrow 2.4-fold range that span what was observed with concatenated constructs previously. Furthermore, the current amplitude data essentially mirror those observed with the dimeric  $\alpha$ -xa- $\beta$  constructs to show that expression levels of functional receptors decrease markedly once total linker lengths are shortened below 25 amino acids. Hence, the  $\gamma$ -11a- $\beta$ - $\alpha$ - $\beta$ - $\alpha$  construct represents a fair direct comparison to the  $\alpha$ -(-1a)- $\beta$ - $\alpha$ - $\gamma$ - $\beta$  construct tested in the previous section and both have total linker lengths of 26 amino acids in their first linker. Judged by the difference in GABA potency, pentameric constructs with the  $\gamma$ 2 subunit in the first construct position appear better suited for linker-length optimizations than those with  $\gamma$ 2 in a center position.



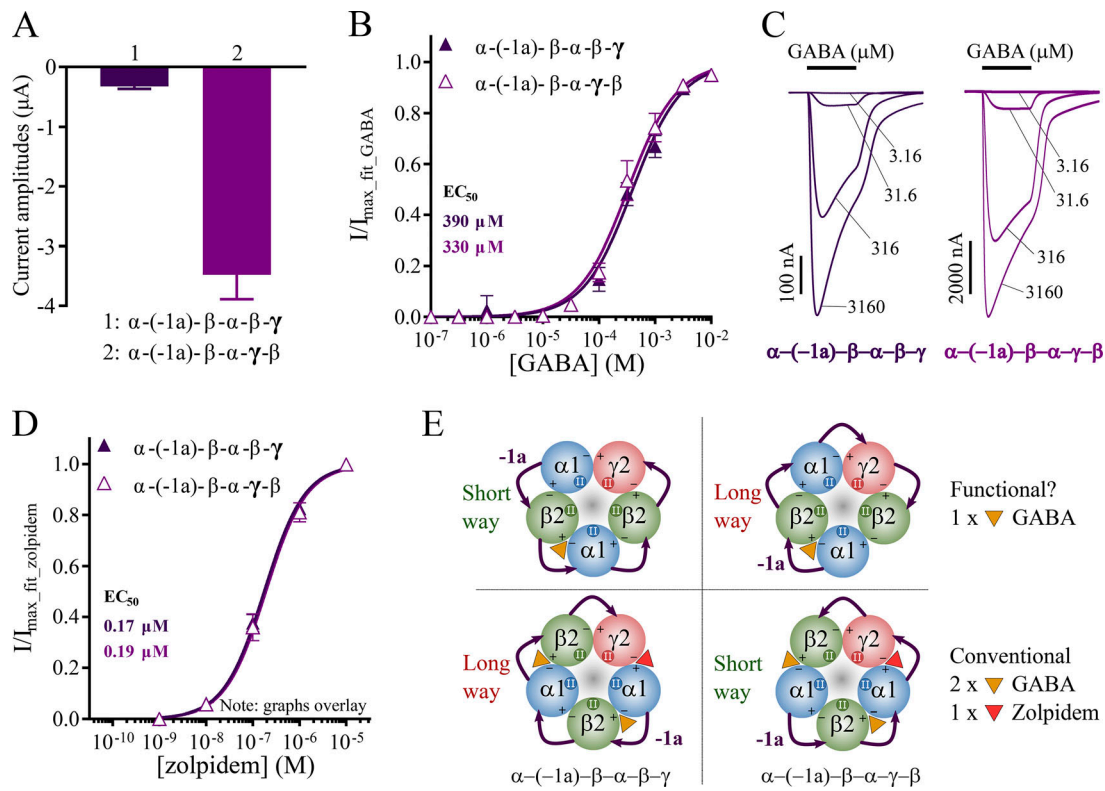


**Figure 8. GABA and zolpidem potency at GABA<sub>A</sub>Rs from concatenated pentameric constructs with a short first linker.** *X. laevis* oocytes were injected with cRNA for the pentameric  $\alpha(-1a)-\beta-\alpha-\beta-\gamma$  or  $\alpha(-1a)-\beta-\alpha-\gamma-\beta$  constructs and subjected to two-electrode voltage-clamp electrophysiology. Electrophysiological data were evaluated as described in the Materials and methods; also see Fig. 1 and Fig. 2. (A) GABA<sub>max</sub>-evoked peak-current amplitudes are depicted as means  $\pm$  SEM for receptors from the indicated cRNA mixtures. A GABA concentration of 316 or 1,000  $\mu$ M was used as GABA<sub>max</sub>. Data were obtained from  $n = 10$ –12 experiments and calculated averages are presented in Table 1. (B) GABA CRRs are depicted as means  $\pm$  SD for receptors from the indicated cRNA mixtures. Data were obtained from  $n = 10$ –12 experiments and regression results are presented in Table 1. (C) Representative traces illustrating GABA CRRs at receptors from the indicated cRNA. Bars above the traces designate the 30-s application time and concentrations of applied GABA are indicated for each trace. (D) Zolpidem enhancement CRRs are depicted as means  $\pm$  SD for the indicated receptors. Data were from  $n = 6$ –12 experiments and regression results are presented in Table 2. (E) Potential receptor assemblies arising from injection of the two pentameric constructs. The respective pentamers can assemble with all linkers in either the clockwise or the counterclockwise orientation. Only one of these assemblies leads to receptors with two canonical GABA-binding  $\beta 2$ - $\alpha 1$  interfaces and a zolpidem-binding  $\alpha 1$ - $\gamma 2$  interface (lower panels). A functional  $\alpha(-1a)-\beta-\alpha-\beta-\gamma$  pentamer requires its linkers to assemble in the longer clockwise orientation (Long way), whereas a functional  $\alpha(-1a)-\beta-\alpha-\gamma-\beta$  pentamer assembles with its linkers in the shorter counterclockwise orientation (Short way).

**Does a pentameric construct ensure a uniform receptor pool?**

An important point to consider when working with concatenated pentameric constructs is whether resultant receptors are actually as expected. It might, for example, be speculated that linker proteolysis could lead to the existence of shorter contaminating concatemers or even free subunits inside oocytes. Fortunately, several studies of pentameric nAChR concatemers have shown that linker proteolysis is not a problem for constructs where the signal peptides are omitted for all but the first subunit (Carbone et al., 2009; Kuryatov and Lindstrom, 2011). Nevertheless, other avenues could still lead to expression of undesired receptors. The open-reading frame for a pentameric GABA<sub>A</sub>R construct is in the vicinity of 7,000 bp. Despite optimization of the experimental conditions for long transcripts, it remains possible that premature termination during cRNA synthesis could lead to pollutant incomplete cRNA entities. Partial degradation of cRNA inside oocytes could potentially give the same result. Concatemers from such incomplete cRNA entities might then assemble with each other or even with

full-length concatemers to give unexpected receptors with dangling subunits.

To investigate whether receptors originate from full-length concatemers we created a new  $\gamma 11a-\beta-\alpha-\beta-\alpha^{R67A}$  construct. The  $\alpha 1^{R67}$  loop D residue represents an important GABA-binding arginine residue in a wild-type  $\beta 2$ - $\alpha 1$  interface (Bergmann et al., 2013). Previous coexpression of rat  $\alpha 1^{R66C}$  (R66 in rat  $\alpha 1$  corresponds to R67 in human  $\alpha 1$ ) or human  $\alpha 1^{R67A}$  with  $\beta 2$  subunits led to a substantial loss in GABA potency from a 6–80- $\mu$ M range to a 1–30-mM range (Boileau et al., 1999; Goldschen-Ohm et al., 2011). The new  $\gamma 11a-\beta-\alpha-\beta-\alpha^{R67A}$  construct contains both a wild-type and a mutant  $\alpha 1$  subunit, and hence full-length concatemers have both a wild-type  $\beta 2$ - $\alpha 1$  and a mutant  $\beta 2$ - $\alpha 1^{R67A}$  GABA-binding site. The two sites have different affinity for GABA; however, as GABA binding in both sites is a requirement for efficient receptor activation, resultant functional GABA potency should only represent binding to the lower-affinity  $\beta 2$ - $\alpha 1^{R67A}$  site. Thus, receptors derived from a single concatemer are expected to have low 1–3-mM GABA

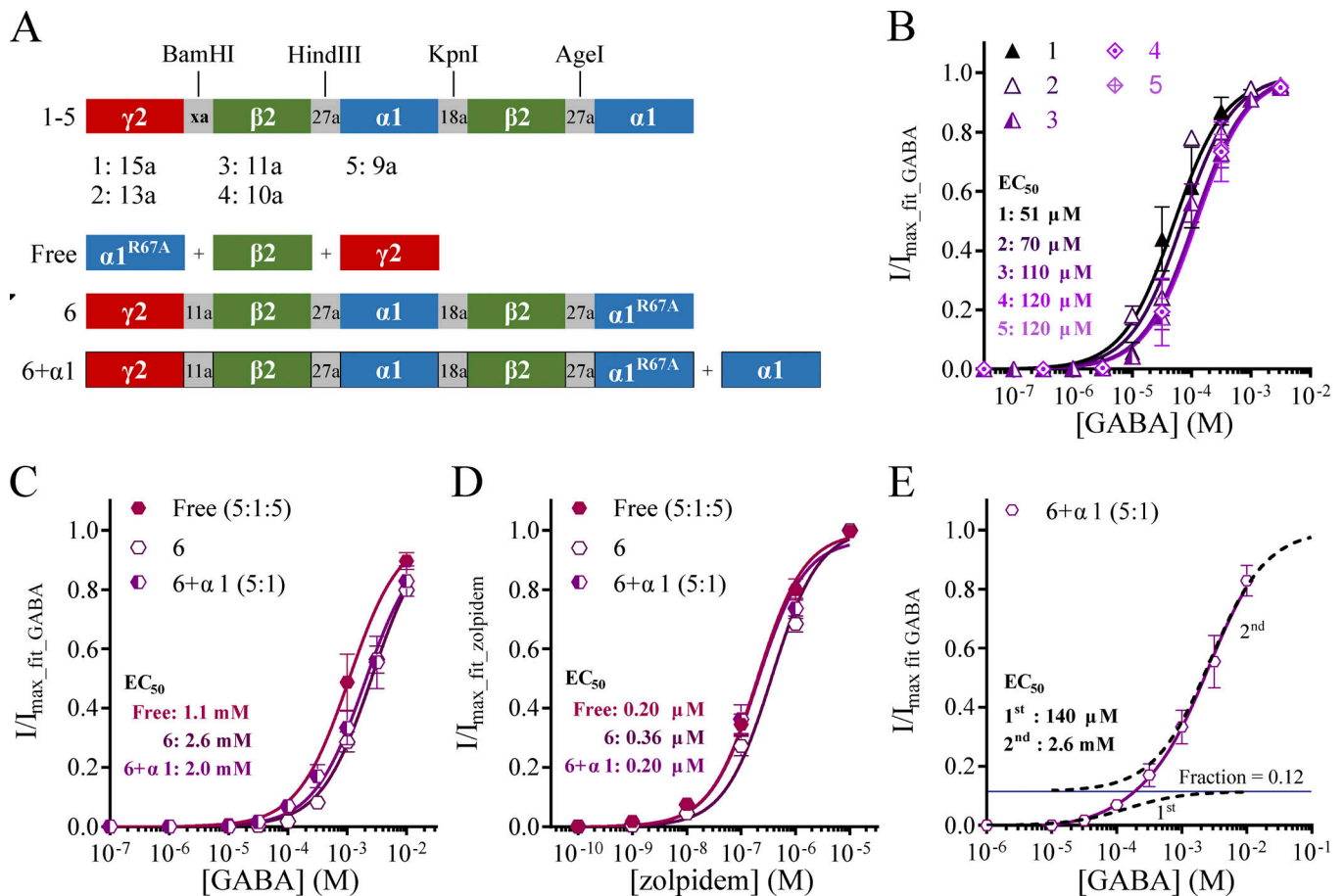


Figure 9. **Design of new concatenated constructs and associated GABA potencies.** *X. laevis* oocytes were injected with cRNA for the indicated pentameric constructs termed 1–6,  $\alpha 1^{R67A}$  +  $\beta 2$  +  $\gamma 2$  in a 5:1:5 ratio or construct 6 +  $\alpha 1$  in a 5:1 ratio and subjected to two-electrode voltage-clamp electrophysiology. Electrophysiological data were evaluated as described in the Materials and methods; also see Fig. 1 and Fig. 2. (A) Pentameric constructs with the  $\gamma 2$  subunit in the first construct position were designed to contain a unique restriction site in each of the four linkers. Whereas the total linker lengths of the first linker for constructs 1–5 were 30, 28, 26, 25, and 24 amino acids, respectively, the remaining three linkers had total lengths of 45 amino acids as presented in Table 3. Construct 6 contained a point-mutated  $\alpha 1^{R67A}$  subunit in the fifth construct position. (B and C) GABA CRRs are depicted as means  $\pm$  SD for receptors from the indicated cRNA mixtures. Data were obtained from  $n = 10$ –17 experiments and regression results are presented in Table 1. (D) Zolpidem enhancement CRRs are depicted as means  $\pm$  SD for the indicated receptors. Data were from  $n = 7$ –11 experiments and regression results are presented in Table 2. (E) GABA CRR data for the 6 +  $\alpha 1$  cRNA mixture from C were re-evaluated and a second-order equation represented the best fit as determined by an F test [ $F_{(1,77)} = 10.1$ ,  $P = 0.0022$ ]. The fraction of the highest potency component was 0.12 and the derived potencies are indicated in the panel. Besides the biphasic graph fitted to the actual data, two simulated graphs are added (dotted black lines) to represent each of the two components determined by the fitting routine.

potency, whereas receptors originating from mixtures of incomplete concatemers missing the  $\alpha 1^{R67A}$  subunit would be expected to have normal  $\sim 100$ - $\mu$ M GABA potency.

Corroborating previous data, coexpression of free  $\alpha 1^{R67A}$ ,  $\beta 2$ , and  $\gamma 2$  subunits in a 5:1:5 biased ratio gave rise to receptors that had a GABA EC<sub>50</sub> value of 1.1 mM (Fig. 9 C and Table 1). However, with average maximal GABA-evoked current amplitudes of 7.1  $\mu$ A and a zolpidem potency of 0.20  $\mu$ M, the mutated  $\alpha 1^{R67A}$  subunit appeared to have no bearing on expression efficiency or zolpidem binding (Fig. 9 D, Table 1, and Table 2). Injection of the  $\gamma$ -11a- $\beta$ - $\alpha$ - $\beta$ - $\alpha^{R67A}$  construct led to similar observations with an average maximal GABA-evoked current amplitude of 3.6  $\mu$ A, a GABA EC<sub>50</sub> value of 2.6 mM, and a zolpidem EC<sub>50</sub> value of 0.36  $\mu$ M (Fig. 9, C and D; Table 1; and Table 2). As expected, the functional potency of GABA is dictated by the lower-affinity  $\beta 2$ - $\alpha 1^{R67A}$  site, and data for this

construct are fully consistent with a uniform receptor pool of  $\beta 2\alpha 1^{R67A}\gamma$  receptors.

In a final experiment, cRNA for  $\gamma$ -11a- $\beta$ - $\alpha$ - $\beta$ - $\alpha^{R67A}$  and wild-type  $\alpha 1$  was mixed in a 5:1 ratio. Assuming equally efficient protein translation, this ratio should give similar copy numbers of concatemers and free  $\alpha 1$  subunits inside oocytes. The GABA and zolpidem CRRs for this mixture had an EC<sub>50</sub> value of 2.0 mM and 0.20  $\mu$ M, respectively, which appears similar to the values observed for  $\gamma$ -11a- $\beta$ - $\alpha$ - $\beta$ - $\alpha^{R67A}$  alone (Fig. 9, C and D; Table 1; and Table 2). Yet, despite similar zolpidem potencies, the observed modulatory efficacy at the 5:1 mixture was  $190\% \pm 4\%$ ,  $n = 9$ , which is threefold lower than the  $580\% \pm 10\%$ ,  $n = 11$ , for the concatemer alone. Given the apparent similar GABA potency and identical conditions in the zolpidem modulator experiments, this suggests that the 5:1 pool contains a population of receptors that does not respond efficiently to zolpidem under these

conditions. Further analysis revealed that while the GABA CRR data for  $\gamma$ -11a- $\beta$ - $\alpha$ - $\beta$ - $\alpha^{R67A}$  alone could only be fitted by a single-order equation (second-order fit ambiguous), those for  $\gamma$ -11a- $\beta$ - $\alpha$ - $\beta$ - $\alpha^{R67A} + \alpha 1$  were best approximated by second-order fitting [ $F_{(1,77)} = 10.1$ ,  $P = 0.0022$ ]. Approximately 12% of the recorded current came from receptors with an  $EC_{50}$  value of 140  $\mu$ M and the remaining 88% from receptors with an  $EC_{50}$  value of 2.6 mM (Fig. 9 E). The receptors with an estimated GABA potency of 140  $\mu$ M obviously lack the  $\alpha 1^{R67A}$  subunit and most likely originate from pentameric concatemers assembled with a free  $\alpha 1$  subunit, leaving a dangling  $\alpha 1^{R67A}$  subunit or incomplete concatemers assembled. Nevertheless, with the GABA<sub>control</sub> concentration of 100  $\mu$ M used in the zolpidem experiments, these receptors would be  $\sim$ 50% activated and respond relatively little to additions of zolpidem.

Overall, these data suggest that when the pentameric  $\gamma$ -11a- $\beta$ - $\alpha$ - $\beta$ - $\alpha^{R67A}$  construct is injected by itself, the resultant receptor pool contains a uniform receptor population. This does not fully exclude the possible existence of minute populations of contaminating receptors, such as di-pentamers with dangling subunits; however, if present, these appear to be negligible. In the experiment with the mixture of  $\gamma$ -11a- $\beta$ - $\alpha$ - $\beta$ - $\alpha^{R67A} + \alpha 1$ ,  $\sim$ 12% of the total current originated from receptors with two wild-type  $\alpha 1$  subunits. That said, it is important to note that this is an extreme scenario where the copy number of free  $\alpha 1$  subunits matches that of the concatemers. The fact that almost 90% of the receptors originated from only concatemers suggests that inclusion of all five linked subunits is the preferred assembly for pentameric constructs.

## Discussion

The Sigel group published the design of the  $\beta$ -23- $\alpha$  and  $\alpha$ -10- $\beta$  constructs in 2001 followed by additional construct designs to include a  $\gamma 2$  subunit in 2002 (Baumann et al., 2001, 2002). Since then, these constructs have set precedence for how to concatenate GABA<sub>A</sub>Rs. The determined linkers were considered optimal and a scheme for how to calculate linker lengths for new constructs was devised (Minier and Sigel, 2004). Furthermore, these studies were accompanied with receptor illustrations, in which the linked subunits were drawn as assembling in a counterclockwise orientation when viewed from the extracellular space.

Initially, we tested resultant receptors from injections of the original  $\beta$ -23- $\alpha$  and  $\alpha$ -10- $\beta$  constructs by themselves or in combination with a monomeric  $\beta 2$  or  $\gamma 2$  subunit and our data generally match the original findings of Baumann et al. (2001), with one notable exception. When injected alone, both constructs gave rise to substantial GABA-evoked currents in our experiments. This was not reported originally, although careful examination of the data in Baumann et al. (2001) reveals low levels of dimer-only expression. Later publications from the Sigel group also note the existence of functional receptors from expression of dimeric constructs by themselves (Kaur et al., 2009; Sigel et al., 2009; Baur and Sigel, 2017). Nevertheless, the key point is that dimers from both constructs assembled readily into fully functional receptors, likely with dangling

subunits (Fig. 3 A). This is important when interpreting data from experiments where dimeric constructs are mixed with free subunits or other concatenated constructs. With the possibility of dangling subunits in the equation, a resultant receptor pool could contain additional unanticipated receptors.

While our data for  $\beta$ -23- $\alpha$  and  $\alpha$ -10- $\beta$  resemble the original findings in Baumann et al. (2001), our view of how these data should associate with schematic receptor drawings differs substantially. To account for the observation that both the  $\beta$ -23- $\alpha + \gamma 2$  and  $\alpha$ -10- $\beta + \gamma 2$  combinations give rise to receptors that are essentially identical with respect to both GABA and zolpidem CRRs, the  $\beta$ -23- $\alpha$  concatemer has to adopt the counterclockwise orientation (Fig. 3 B, receptor 1), whereas the  $\alpha$ -10- $\beta$  has to adopt the clockwise orientation to form a receptor with two GABA-binding interfaces and one zolpidem-binding interface (Fig. 3 B, receptor 4). Our conclusion is therefore that these two dimers assemble in opposite orientations when coexpressed with a  $\gamma 2$  subunit to form canonical GABA<sub>A</sub>Rs. To substantiate this, we created two new concatenated tetrameric constructs based on  $\alpha$ -10- $\beta$ . As expected, functional receptors assembled readily with the linked tetramers in opposite orientations depending on the specific subunit order within the construct (Fig. 4 E).

We recently demonstrated that long linkers in published concatenated dimeric nAChR constructs result in subunit assembly in both the clockwise and the counterclockwise orientations (Ahring et al., 2018). The linkers of  $\beta$ -23- $\alpha$  and  $\alpha$ -10- $\beta$  likewise appear sufficiently long to allow a similar situation for GABA<sub>A</sub>Rs. Based on studies of 3D structures of Cys-loop receptors, the counterclockwise orientation should, however, represent the shortest way for a linker. Therefore, in an attempt to constrain assembly to a predominant counterclockwise orientation, we created a range of new dimeric  $\alpha$ - $\beta$  constructs. These were expressed alone or coexpressed with free  $\beta 2$  or  $\gamma 2$  subunits. Two key observations emerged from these experiments. First, expression of functional dimer-only receptors with dangling subunits appear less prominent as the linker is shortened, which certainly is desirable as such receptors may cloud interpretation of functional data. Second, identification of a linker length that would restrict assembly of dimers to the counterclockwise orientation required substantial optimization, and only the  $\alpha$ -(-1a)- $\beta$  and  $\alpha$ -(-2a)- $\beta$  constructs resulted in the desired outcome.

There are numerous published studies where schematic drawings of concatenated receptors have been associated with functional data for monomeric, dimeric, and trimeric construct combinations. Given that many of these constructs can give rise to receptors with dangling subunits and that the orientation of concatemers can change depending on the circumstances, the respective conclusions may be erroneous. For example, Botzolakis et al. (2016) proposed several novel receptor GABA<sub>A</sub>R stoichiometries and, among these, one where a  $\gamma$  subunit substitutes for a  $\beta$  subunit to give a  $\beta\alpha\gamma\alpha\gamma$  receptor (viewed counterclockwise from the extracellular space). This non-canonical receptor assembly was suggested based on receptors formed from expressing a dimeric  $\alpha$ - $\gamma$  construct with free  $\beta$  subunits. However, in light of our data, the receptors formed could simply include two dimers and two free  $\beta$  subunits in a canonical  $\beta\alpha\beta\alpha\gamma$

assembly with a dangling  $\gamma$  subunit. This seems a rather likely explanation and similar scenarios have been demonstrated for nAChRs (Groot-Kormelink et al., 2004). In another example, Kaur et al. (2009) suggested that a GABA<sub>A</sub>R  $\delta$  subunit can substitute for the  $\alpha$ -subunit to give a GABA-binding  $\beta$ - $\delta$  interface. This was evidenced by coexpressing a mixture of concatenated  $\alpha$ - $\beta$ - $\alpha$  and  $\beta$ - $\delta$  constructs and associating the data with a schematic drawing of an  $\alpha\beta\alpha\beta\delta$  receptor. However, if the  $\beta$ - $\delta$  dimer assembled in the opposite orientation, the resulting receptor would have a  $\beta\beta\alpha\delta$  stoichiometry with two canonical  $\beta$ - $\alpha$  GABA-binding interfaces.

In light of all the potential issues observed with mixtures of dimeric constructs and free subunits, we sought to make pentameric constructs with restricted assembly orientation to evaluate their utility for future studies. By extending the already optimized  $\alpha$ -(-1a)- $\beta$  dimeric construct it proved possible to obtain new constructs for which assembly clearly favored the counterclockwise orientation. This was demonstrated by designing two constructs, such that functional receptors must arise from assembly in opposite orientations: clockwise for  $\alpha$ -(-1a)- $\beta$ - $\alpha$ - $\beta$ - $\gamma$  and counterclockwise for  $\alpha$ -(-1a)- $\beta$ - $\alpha$ - $\gamma$ - $\beta$ . Although receptors for the two constructs appeared functionally identical, the one designed for counterclockwise assembly resulted, as expected, in 11-fold greater current amplitudes. However, much to our surprise, this came with an  $\sim$ 10-fold shift in GABA potency and therefore a set of five new constructs were created. These had the  $\gamma$ 2 subunit in the first construct position and different first linker lengths ( $\gamma$ -xa- $\beta$ - $\alpha$ - $\beta$ - $\alpha$ ). With respect to GABA potency, these constructs all appeared within the normal range and are therefore superior in comparison with the  $\alpha$ -(-1a)- $\beta$ - $\alpha$ - $\gamma$ - $\beta$  construct. Depending on the specific need, one or more of these constructs would therefore be well suited for future studies.

In a final set of experiments, we investigated whether resultant receptors from a pentameric construct with a short first linker are actually the ones expected. Obviously, a pentameric construct contains four linkers of which only the first linker length was optimized in our constructs. Hence, it is plausible that contaminating incomplete concatemers could assemble with each other or with full-length concatemers to create functional receptors with dangling subunits. With linkers 2–4 being longer than linker 1, dangling could occur in any of these positions; however, for steric reasons, it appears improbable that dangling would only involve one or two of the middle subunits. If dangling occurs, it would be expected to always include the subunit on the fifth position. Thus, we created a construct with a reporter R67A mutation in the fifth construct position  $\alpha$ 1 subunit ( $\gamma$ -11a- $\beta$ - $\alpha$ - $\beta$ - $\alpha$ <sup>R67A</sup>). The  $\alpha$ 1<sup>R67A</sup> mutation lowers the GABA potency of resultant mutant receptors by  $\sim$ 50-fold, thereby making it obvious if a receptor pool contains wild-type receptors along with mutant receptors. Data with this mutant construct demonstrated that when the pentameric construct was injected by itself, the receptor pool appeared uniform for all practical purposes.

The large number of GABA<sub>A</sub>R subunits and their ability to assemble in many stoichiometries represent a substantial challenge in the field. Recent publications suggesting that  $\alpha$ ,  $\beta$ , and  $\gamma$

subunits are interchangeable have only added to the existing knowledge chaos (Baur et al., 2009, 2010; Kaur et al., 2009; Botzolakis et al., 2016; Wongsamitkul et al., 2017). However, we speculate that many of these findings may not hold true once revisited. In our studies with coexpression of  $\alpha$ -xa- $\beta$  dimers with  $\gamma$ 2, we observed a three- to fourfold lower GABA potency at  $\alpha$ -0a- $\beta$  +  $\gamma$ 2. In the simplest scenarios, this cRNA combination can give rise to three possible receptor combinations: the conventional  $\beta\alpha\beta\alpha\gamma$  receptor and two rearranged stoichiometries,  $\beta\alpha\beta\gamma\alpha$  and  $\beta\beta\alpha\gamma\alpha$ , thereof (Fig. 3 B; receptor 4, 5, and 6, respectively). Given that  $\beta\gamma$  receptors have been proposed to be fully functional with GABA potencies in the micromolar range (Whittemore et al., 1996; Chua et al., 2015; Wongsamitkul et al., 2017), we were interested in evaluating whether a  $\beta\alpha\beta\gamma\alpha$  receptor (Fig. 3 B, receptor 5), with its canonical GABA-binding  $\beta$ - $\alpha$  interface and a potential GABA-binding  $\beta$ - $\gamma$  interface, represents a functional constituent in the receptor pool. Introduction of a key arginine (corresponding to  $\alpha$ 1<sup>R67</sup>) in the complementary face of the  $\gamma$ 2 subunit, however, revealed no evidence that  $\beta$ - $\gamma$  interfaces participate in GABA-mediated activation in these experiments. Hence, despite optimal conditions for formation of a functional  $\beta\alpha\beta\gamma\alpha$  receptor, no evidence of its existence was noted.

High-affinity GABA binding to the  $\beta$ - $\alpha$  interface is dependent on specific determinants residing on both the principal  $\beta$  and the complementary  $\alpha$  face. The most important include the aromatic box residues and the key arginine residue corresponding to  $\alpha$ 1<sup>R67</sup> as shown previously (Bergmann et al., 2013). All  $\alpha$  subunits have an arginine in this position as also do the  $\pi$  and  $\rho$  subunits; however,  $\beta$ ,  $\gamma$ , and  $\delta$  subunits do not. GABA can certainly bind in interfaces that lack this arginine as exemplified by expression of  $\beta$ 3 homomers in oocytes (Chua et al., 2015) and by our experiments with the  $\gamma$ -11a- $\beta$ - $\alpha$ - $\beta$ - $\alpha$ <sup>R67A</sup> construct, albeit with a significant loss in potency. For the homomeric  $\beta$ 3 receptor, GABA activation occurs at concentrations in excess of 10 mM and we observed potencies in the 1–3-mM range for  $\gamma$ -11a- $\beta$ - $\alpha$ - $\beta$ - $\alpha$ <sup>R67A</sup>. We therefore suggest that it is unlikely that  $\beta$ - $\beta$ ,  $\beta$ - $\gamma$ , or  $\beta$ - $\delta$  interfaces contribute to GABA activation of a receptor within a normal 1- $\mu$ M to 1-mM concentration range. Hence, the chaos surrounding GABA<sub>A</sub>R assembly may actually be less chaotic than recent data seem to suggest.

### Conclusion and future directions

Our data emphasize that great care should be taken when interpreting data based on the widely used concatenated constructs, especially where they are associated with oversimplified schematic drawings of a GABA<sub>A</sub>R. Fortunately, our data demonstrate that it is possible to optimize constructs such that concatemer assembly is restricted to the counterclockwise orientation, albeit this might require substantial efforts depending on the need and the specific subunits involved. A striking lesson was the complexity associated with the use of dimeric constructs, since a fine-tuning effort involves combatting not only the assembly orientation possibilities but also the inherent ability for assembly with dangling subunits. Hence, our data suggest that pentameric constructs should be used for applications that require a high degree of control over the assembly



process. Finally, while our work presents a way forward, there is still room for further refinement. Pentameric constructs contain four linkers and while we have addressed the first, it seems logical to also pay attention to the other three linkers in future constructs. Although less-flexible linkers in more positions would likely increase the probability of obtaining only the desired receptors, shortening of the last linker seems an obvious avenue as that can potentially also limit dangling of the fifth subunit.

## Acknowledgments

This work was supported by the Australian Research Council (LP160100560) and the Australian National Health and Medical Research Council (APP1124567 and APP1081733 to M. Chebib, P.K. Ahring, and T. Balle). N.M. Kowal was supported by the Icelandic Research Fund (grant number 152604).

The authors declare no competing financial interests.

Author contributions: P.K. Ahring designed the research; V.W.Y. Liao, P.K. Ahring, H.C. Chua, N.M. Kowal, and T. Balle performed the research; P.K. Ahring analyzed the data and wrote the manuscript. P.K. Ahring, T. Balle, and M. Chebib acquired the necessary funding. All authors approved the final version of the manuscript.

Richard W. Aldrich served as editor.

Submitted: 25 May 2018

Accepted: 20 March 2019

## References

- Ahring, P.K., L.H. Bang, M.L. Jensen, D. Strøbæk, L.Y. Hartiadi, M. Chebib, and N. Absalom. 2016. A pharmacological assessment of agonists and modulators at  $\alpha 4\beta 2\gamma 2$  and  $\alpha 4\beta 2\delta$  GABAA receptors: The challenge in comparing apples with oranges. *Pharmacol. Res.* 111:563–576. <https://doi.org/10.1016/j.phrs.2016.05.014>
- Ahring, P.K., V.W.Y. Liao, and T. Balle. 2018. Concatenated nicotinic acetylcholine receptors: A gift or a curse? *J. Gen. Physiol.* 150:453–473.
- Angelotti, T.P., and R.L. Macdonald. 1993. Assembly of GABAA receptor subunits: alpha 1 beta 1 and alpha 1 beta 1 gamma 2S subunits produce unique ion channels with dissimilar single-channel properties. *J. Neurosci.* 13: 1429–1440. <https://doi.org/10.1523/JNEUROSCI.13-04-01429.1993>
- Baumann, S.W., R. Baur, and E. Sigel. 2001. Subunit arrangement of gamma-aminobutyric acid type A receptors. *J. Biol. Chem.* 276:36275–36280. <https://doi.org/10.1074/jbc.M105240200>
- Baumann, S.W., R. Baur, and E. Sigel. 2002. Forced subunit assembly in  $\alpha 1\beta 2\gamma 2$  GABAA receptors. Insight into the absolute arrangement. *J. Biol. Chem.* 277:46020–46025. <https://doi.org/10.1074/jbc.M207663200>
- Baumann, S.W., R. Baur, and E. Sigel. 2003. Individual properties of the two functional agonist sites in GABA(A) receptors. *J. Neurosci.* 23: 11158–11166. <https://doi.org/10.1523/JNEUROSCI.23-35-11158.2003>
- Baur, R., and E. Sigel. 2017. Low expression in *Xenopus* oocytes and unusual functional properties of  $\alpha 1\beta 2\gamma 2$  GABAA receptors with non-conventional subunit arrangement. *PLoS One.* 12:e0170572. <https://doi.org/10.1371/journal.pone.0170572>
- Baur, R., F. Miniér, and E. Sigel. 2006. A GABA(A) receptor of defined subunit composition and positioning: concatenation of five subunits. *FEBS Lett.* 580:1616–1620. <https://doi.org/10.1016/j.febslet.2006.02.002>
- Baur, R., K.H. Kaur, and E. Sigel. 2009. Structure of alpha6 beta3 delta GABA(A) receptors and their lack of ethanol sensitivity. *J. Neurochem.* 111: 1172–1181. <https://doi.org/10.1111/j.1471-4159.2009.06387.x>
- Baur, R., K.H. Kaur, and E. Sigel. 2010. Diversity of structure and function of  $\alpha 1\alpha 6\beta 3\delta$  GABAA receptors: Comparison with  $\alpha 1\beta 3\delta$  and  $\alpha 6\beta 3\delta$  receptors. *J. Biol. Chem.* 285:17398–17405. <https://doi.org/10.1074/jbc.M110.108670>
- Bergmann, R., K. Kongsbak, P.L. Sørensen, T. Sander, and T. Balle. 2013. A unified model of the GABA(A) receptor comprising agonist and benzodiazepine binding sites. *PLoS One.* 8:e52323. <https://doi.org/10.1371/journal.pone.0052323>
- Boileau, A.J., A.R. Evers, A.F. Davis, and C. Czajkowski. 1999. Mapping the agonist binding site of the GABAA receptor: evidence for a beta-strand. *J. Neurosci.* 19:4847–4854. <https://doi.org/10.1523/JNEUROSCI.19-12-04847.1999>
- Boileau, A.J., R.A. Pearce, and C. Czajkowski. 2005. Tandem subunits effectively constrain GABAA receptor stoichiometry and recapitulate receptor kinetics but are insensitive to GABAA receptor-associated protein. *J. Neurosci.* 25:11219–11230. <https://doi.org/10.1523/JNEUROSCI.3751-05.2005>
- Botzolakis, E.J., K.N. Gurba, A.H. Lagrange, H.J. Feng, A.K. Stanic, N. Hu, and R.L. Macdonald. 2016. Comparison of  $\gamma$ -aminobutyric acid, type A (GABAA), receptor  $\alpha\beta\gamma$  and  $\alpha\beta\delta$  expression using flow cytometry and electrophysiology. *J. Biol. Chem.* 291:20440–20461. <https://doi.org/10.1074/jbc.M115.698860>
- Bracamontes, J.R., and J.H. Steinbach. 2009. Steroid interaction with a single potentiating site is sufficient to modulate GABA-A receptor function. *Mol. Pharmacol.* 75:973–981. <https://doi.org/10.1124/mol.108.053629>
- Carbone, A.L., M. Moroni, P.J. Groot-Kormelink, and I. Bermudez. 2009. Pentameric concatenated (alpha4)(2)(beta2)(3) and (alpha4)(3)(beta2)(2) nicotinic acetylcholine receptors: subunit arrangement determines functional expression. *Br. J. Pharmacol.* 156:970–981. <https://doi.org/10.1111/j.1476-5381.2008.00104.x>
- Che Has, A.T., N. Absalom, P.S. van Nieuwenhuijzen, A.N. Clarkson, P.K. Ahring, and M. Chebib. 2016. Zolpidem is a potent stoichiometry-selective modulator of  $\alpha 1\beta 3$  GABAA receptors: Evidence of a novel benzodiazepine site in the  $\alpha 1$ - $\alpha 1$  interface. *Sci. Rep.* 6:28674. <https://doi.org/10.1038/srep28674>
- Chua, H.C., and M. Chebib. 2017. GABA<sub>A</sub> receptors and the diversity in their structure and pharmacology. *Adv. Pharmacol.* 79:1–34. <https://doi.org/10.1016/bs.apha.2017.03.003>
- Chua, H.C., N.L. Absalom, J.R. Hanrahan, R. Viswas, and M. Chebib. 2015. The direct actions of GABA, 2'-methoxy-6-methylflavone and general anaesthetics at  $\beta 3\gamma 2L$  GABAA receptors: Evidence for receptors with different subunit stoichiometries. *PLoS One.* 10:e0141359. <https://doi.org/10.1371/journal.pone.0141359>
- Eriksen, S.S., and A.J. Boileau. 2007. Tandem cointer: Cys-loop receptor concatamer insights and caveats. *Mol. Neurobiol.* 35:113–127. <https://doi.org/10.1007/BF02700627>
- Goldschen-Ohm, M.P., D.A. Wagner, and M.V. Jones. 2011. Three arginines in the GABAA receptor binding pocket have distinct roles in the formation and stability of agonist- versus antagonist-bound complexes. *Mol. Pharmacol.* 80:647–656. <https://doi.org/10.1124/mol.111.072033>
- Groot-Kormelink, P.J., S.D. Broadbent, J.P. Boonman, and L.G. Sivillotti. 2004. Incomplete incorporation of tandem subunits in recombinant neuronal nicotinic receptors. *J. Gen. Physiol.* 123:697–708. <https://doi.org/10.1085/jgp.200409042>
- Hartiadi, L.Y., P.K. Ahring, M. Chebib, and N.L. Absalom. 2016. High and low GABA sensitivity  $\alpha 4\beta 2\delta$  GABAA receptors are expressed in *Xenopus* laevis oocytes with divergent stoichiometries. *Biochem. Pharmacol.* 103: 98–108. <https://doi.org/10.1016/j.bcp.2015.12.021>
- Im, W.B., J.F. Pregonzer, J.A. Binder, G.H. Dillon, and G.L. Alberts. 1995. Chloride channel expression with the tandem construct of alpha 6-beta 2 GABAA receptor subunit requires a monomeric subunit of alpha 6 or gamma 2. *J. Biol. Chem.* 270:26063–26066. <https://doi.org/10.1074/jbc.270.44.26063>
- Kaur, K.H., R. Baur, and E. Sigel. 2009. Unanticipated structural and functional properties of delta-subunit-containing GABAA receptors. *J. Biol. Chem.* 284:7889–7896. <https://doi.org/10.1074/jbc.M806484200>
- Kowal, N.M., P.K. Ahring, V.W.Y. Liao, D.C. Indurtti, B.S. Harvey, S.M. O'Connor, M. Chebib, E.S. Olafsdottir, and T. Balle. 2018. Galantamine is not a positive allosteric modulator of human  $\alpha 4\beta 2$  or  $\alpha 7$  nicotinic acetylcholine receptors. *Br. J. Pharmacol.* 175:2911–2925. <https://doi.org/10.1111/bph.14329>
- Kuryatov, A., and J. Lindstrom. 2011. Expression of functional human  $\alpha 6\beta 2\beta 3^*$  acetylcholine receptors in *Xenopus* laevis oocytes achieved through subunit chimeras and concatamers. *Mol. Pharmacol.* 79: 126–140. <https://doi.org/10.1124/mol.110.066159>
- Lee, H.J., N.L. Absalom, J.R. Hanrahan, P. van Nieuwenhuijzen, P.K. Ahring, and M. Chebib. 2016. A pharmacological characterization of GABA, THIP and DS2 at binary  $\alpha 4\beta 3$  and  $\beta 3\delta$  receptors: GABA activates  $\beta 3\delta$

- receptors via the  $\beta 3(+)\delta(-)$  interface. *Brain Res.* 1644:222–230. <https://doi.org/10.1016/j.brainres.2016.05.019>
- Miller, P.S., and A.R. Aricescu. 2014. Crystal structure of a human GABAA receptor. *Nature.* 512:270–275. <https://doi.org/10.1038/nature13293>
- Minier, F., and E. Sigel. 2004. Techniques: Use of concatenated subunits for the study of ligand-gated ion channels. *Trends Pharmacol. Sci.* 25: 499–503. <https://doi.org/10.1016/j.tips.2004.07.005>
- Mirza, N.R., J.S. Larsen, C. Mathiasen, T.A. Jacobsen, G. Munro, H.K. Erichsen, A.N. Nielsen, K.B. Troelsen, E.O. Nielsen, and P.K. Ahring. 2008. NS11394 [3'-[5-(1-hydroxy-1-methyl-ethyl)-benzoimidazol-1-yl]-biphenyl-2-carbonitrile], a unique subtype-selective GABAA receptor positive allosteric modulator: in vitro actions, pharmacokinetic properties and in vivo anxiolytic efficacy. *J. Pharmacol. Exp. Ther.* 327: 954–968. <https://doi.org/10.1124/jpet.108.138859>
- Mortensen, M., and T.G. Smart. 2006. Extrasynaptic alphabeta subunit GABAA receptors on rat hippocampal pyramidal neurons. *J. Physiol.* 577: 841–856. <https://doi.org/10.1113/jphysiol.2006.117952>
- Olsen, R.W., and W. Sieghart. 2008. International Union of Pharmacology. LXX. Subtypes of gamma-aminobutyric acid(A) receptors: classification on the basis of subunit composition, pharmacology, and function. Update. *Pharmacol. Rev.* 60:243–260. <https://doi.org/10.1124/pr.108.005050>
- Shu, H.J., J. Bracamontes, A. Taylor, K. Wu, M.M. Eaton, G. Akk, B. Manion, A.S. Evers, K. Krishnan, D.F. Covey, et al. 2012. Characteristics of concatemeric GABA(A) receptors containing  $\alpha 4/\delta$  subunits expressed in *Xenopus* oocytes. *Br. J. Pharmacol.* 165:2228–2243. <https://doi.org/10.1111/j.1476-5381.2011.01690.x>
- Sigel, E., K.H. Kaur, B.P. Lüscher, and R. Baur. 2009. Use of concatamers to study GABAA receptor architecture and function: application to delta-subunit-containing receptors and possible pitfalls. *Biochem. Soc. Trans.* 37:1338–1342. <https://doi.org/10.1042/BST0371338>
- Söderhielm, P.C., T. Balle, S. Bak-Nyhus, M. Zhang, K.M. Hansen, P.K. Ahring, and A.A. Jensen. 2018. Probing the molecular basis for affinity/potency- and efficacy-based subtype-selectivity exhibited by benzodiazepine-site modulators at GABA<sub>A</sub> receptors. *Biochem. Pharmacol.* 158:339–358. <https://doi.org/10.1016/j.bcp.2018.08.019>
- Whittemore, E.R., W. Yang, J.A. Drewe, and R.M. Woodward. 1996. Pharmacology of the human gamma-aminobutyric acidA receptor alpha 4 subunit expressed in *Xenopus laevis* oocytes. *Mol. Pharmacol.* 50: 1364–1375.
- Wongsamitkul, N., M.C. Maldifassi, X. Simeone, R. Baur, M. Ernst, and E. Sigel. 2017.  $\alpha$  Subunits in GABA<sub>A</sub> receptors are dispensable for GABA and diazepam action. *Sci. Rep.* 7:15498. <https://doi.org/10.1038/s41598-017-15628-7>
- Zhu, S., C.M. Noviello, J. Teng, R.M. Walsh Jr., J.J. Kim, and R.E. Hibbs. 2018. Structure of a human synaptic GABA<sub>A</sub> receptor. *Nature.* 559:67–72. <https://doi.org/10.1038/s41586-018-0255-3>